2016

Examination of a Post-Stroke Drug Treatment for its Effect on Blood Brain Barrier Permeability, and Gene Expression Changes in the Peri-Infarct Region

Ankita Anil Patel
Wright State University

EXAMINATION OF A POST-STROKE DRUG TREATMENT FOR ITS EFFECT ON BLOOD BRAIN BARRIER PERMEABILITY, AND GENE EXPRESSION CHANGES IN THE PERI-INFARCT REGION

A thesis submitted in partial fulfillment of the
requirements for the degree of
Master of Science

By

ANKITA ANIL PATEL
B.S., Western Kentucky University, 2012

2016
Wright State University

WRIGHT STATE UNIVERSITY

GRADUATE SCHOOL

May 27, 2016

I HEREBY RECOMMEND THAT THE THESIS PREPARED UNDER MY SUPERVISION BY Ankita Anil Patel ENTITLED Examination of a Post-Stroke Drug Treatment for its Effect on Blood Brain Barrier Permeability, and Gene Expression Changes in the Peri-infarct Region BE ACCEPTED IN PARTIAL FULFILLMENT OF THE REQUIREMENTS FOR THE DEGREE OF Master of Science.

_____

Adrian Corbett, Ph.D.
Thesis Director

_____

Christopher Wyatt, Ph.D.
Department Chair
Department of Neuroscience, Cell Biology, and Physiology

Committee on
Final Examination

_____
Adrian Corbett, Ph.D.

_____
Debra Mayes, Ph.D.

_____
Salim El-Amouri, Ph.D.

_____
Robert E.W. Fyffe, Ph.D.
Vice President for Research and
Dean of the Graduate School

ABSTRACT

Patel, Ankita Anil. M.S. Department of Neuroscience, Cell Biology, and Physiology, Wright State University, 2016. Examination of a Post-Stroke Drug Treatment for its Effect on Blood Brain Barrier Permeability, and Gene Expression Changes in the Peri-infarct Region.

In this current study, we have investigated a combination of fluoxetine, simvastatin and ascorbic acid administered daily beginning at 20-26 hours after stroke induction. We hope to understand therapeutic abilities by studying its effectiveness on the blood brain barrier permeability and gene expression changes of the microglial subtypes involved in neuro-inflammation and neurogenesis factors in the peri-infarct region. Our results indicate that S-enantiomer of fluoxetine may be more beneficial compared to the R-enantiomer. The S-enantiomer was effective in tightening the blood brain barrier in contrast to the R-enantiomer, in which the latter showed a greater Evans Blue dye permeability across the BBB studied in the cerebral cortex and cerebellum. Similarly, gene expression studies of both enantiomers compared in male and female groups confirmed the presence of microglial subtypes, and the study also showed the S-enantiomer appears to up-regulate neurogenesis growth factors and down-regulate inflammatory signals.

TABLE OF CONTENTS

LIST OF FIGURES

LIST OF TABLES

Table Page

ACKNOWLEDGEMENT

First and foremost, I would like to thank my advisor, Dr. Adrian M. Corbett for her guidance in accomplishing as well as in the development of this project. I appreciate her patience in teaching me the skills and knowledge involved in scientific research. I also appreciate her generosity in investing her time and effort to supervise my thesis work in her laboratory. I would also like to thank my thesis committee members for their contribution of time and effort to provide their suggestions in improvement of this work.

I am also thankful to both of my parents for encouraging me to pursue a master's degree to advance in education, and giving me the freedom to independently explore and personally grow as I pave my way to build a career. I am very grateful for their unconditional love and support, and also appreciate them for providing me with what they could.

I am also very thankful to my senior, Moner A. Ragas, for his mentored student support and sharing of the resources that have helped me to strengthen and sharpen my research skills tremendously.

And lastly, please allow me to extend my acknowledgement to the lovely rats who have perished for the benefit of mankind. I hope their souls are at rest in peace in heaven.

I. INTRODUCTION

Background

In the United States, serious medical implications leading to a long-term disability occur due to a critical medical condition, called stroke. Stroke is the fifth leading cause of death in the US [1]. Each year approximately 795,000 people suffer from stroke, and more than 140,000 stroke-induced deaths occur [2]. Each year about 600,000 people suffer from stroke for the first time, and about 185,000 (31%) have reported repeating attacks [2]. Strokes can occur at any age, however, people over the age of 65 have a greater incidence of stroke when compared to those under 65 (three-fourths to one-fourth respectively). In fact, the risk factor doubles each decade over the age of 55 [3].

Stroke is defined as interruption of blood flow to any area of the brain. This is a major issue because blood flow occlusion can cause oxygen deficiency within minutes. This can trigger the death of brain cells and affect physiological function of parts of the nervous system. There are two known types of stroke: ischemic stroke and hemorrhagic stroke (sub-types: intracerebral hemorrhage and subarachnoid hemorrhage) as shown in figure 1.

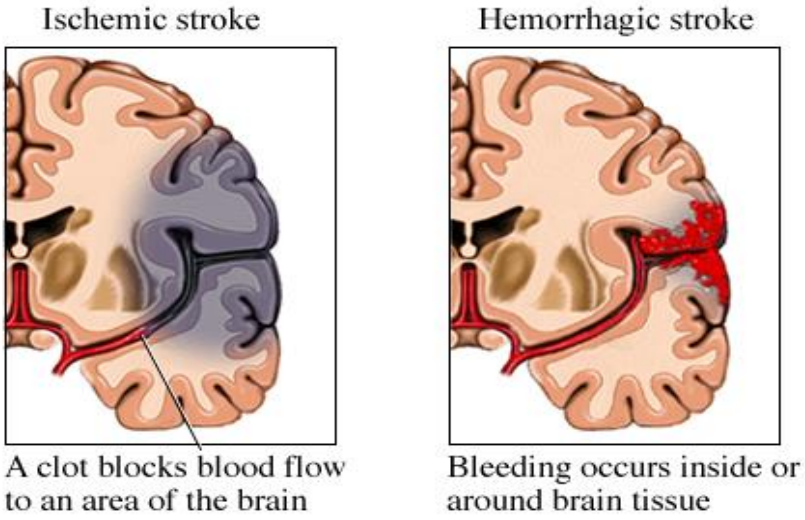

Figure 1 Types of Stroke: Ischemic Stroke and Hemorrhagic Stroke. Pictures courtesy of http://www.wjmc.org/StrokeCare/WJMC-Neuroscience-Types-Of-Stroke.aspx

Ischemic stroke is the most common type of stroke, accounting for approximately 88%, and is caused by arterial occlusion. A warning stroke, often labeled as a 'mini-stroke', is a temporary arterial blockage inside the brain and is called transient ischemic attack (TIA). Its symptoms occur rapidly and persist for less than five minutes, with an average of one minute [2].

Hemorrhagic stroke is caused by a rupture of a blood vessel leading to bleeding inside the brain. The two hemorrhagic stroke sub-types differ in that, following a vessel rupture, in the case of intracerebral hemorrhage, the blood is released into the brain compressing brain structures, whereas in the case of subarachnoid hemorrhage, the blood fills spaces surrounding the brain rather than inside of it.

It is estimated that two-thirds of stroke survivors will have some type of disability [2]. Severity of a disability is dependent on the location of the stroke, which matters more than if the stroke is major or minor. For example, if a large stroke is in the somatosensory region, it wouldn't have a huge functional effect, but if a small stroke is in the motor cortex, the effect will be large. A minor stroke in the motor cortex causes minor problems such as temporary weakness in a limb whereas a major stroke in the same location can cause permanent disabilities such as paralysis on one side of the body. With such known severity of stroke, research dedicated to find an effective treatment is a subject of prime interest.

Currently, treatment available for stroke is intravenous injection of tissue plasminogen activator (tPA), which dissolves the blood clot to restore normal blood flow. However, it poses a risk of causing uncontrollable bleeding inside the brain and the intravenous route renders it effective if tPA is administered within 3 to 4.5 hours of the onset of stroke, with the chance of improvement being greater with earlier treatment [4]. The reason tPA must be administered within this time frame is because after 5 hours it causes bleeding inside the brain, which negates any beneficial effects achieved from blood clot removal. Thrombin in the blood causes neuro-inflammation in the brain which can make the damage from a stroke worse as neuro-inflammation can irritate and destroy normal blood vessels. Hence, this treatment is preferred currently if the patient makes it to the hospital in time, and generally about 73% of stroke victims do not reach the hospital in time to be considered for tPA treatment [5].

Another treatment option is an endovascular procedure called mechanical thrombectomy, which surgically removes the blood clot via insertion of a stent retriever.

This method yields the best functional recovery compared to other treatments, because it surgically removes the whole clot. In addition, its time period for intervention is valid up to 8 hours after stroke onset, which is significantly greater than the time period valid for tPA administration. Results from one study show that 64% of patients with MALCOM (maximal admission lesion volume compatible with favorable outcome) of less than 39 milliliters in size achieved favorable outcome after undergoing thrombectomy [6].

Another known treatment, if stroke victims arrive at the hospital more than 12 hours after stroke, they are administered Aspirin, an acetylsalicylic acid which inhibits COX-1 enzyme, thus preventing platelet aggregation [7].

Although all of these discussed options are effective in removal of the blood clot, they are not completely reliable to treat a stroke condition because they do pose their own disadvantages. Aspirin provides a treatment only temporarily; tPA administration allows a narrow time window for treatment; and a thrombectomy is an invasive procedure to be performed within few hours of the onset of stroke [8]. In fact, *Barber et. al* [5] reports that only about 27% of stroke patients qualified and received intravenous tPA treatment which is a preferred current method. Because of this low percentage, discovery of a compelling post-stroke treatment plan with drugs that can be administered 20-26 hours after the onset of stroke and still yield functional recovery is warranted.

Increasing Neurogenesis Pharmacologically

Current research indicates that the combination of fluoxetine, simvastatin, and ascorbic acid is effective in increasing neurogenesis following stroke survival surgery in rat models [9]. Fluoxetine (brand name Prozac) is an antidepressant of the selective serotonin reuptake inhibitor (SSRI) family, which has been shown to increase

neurogenesis in adult rat models [10]. Figure 2 indicates the organic structure of fluoxetine and its R- and S-enantiomers.

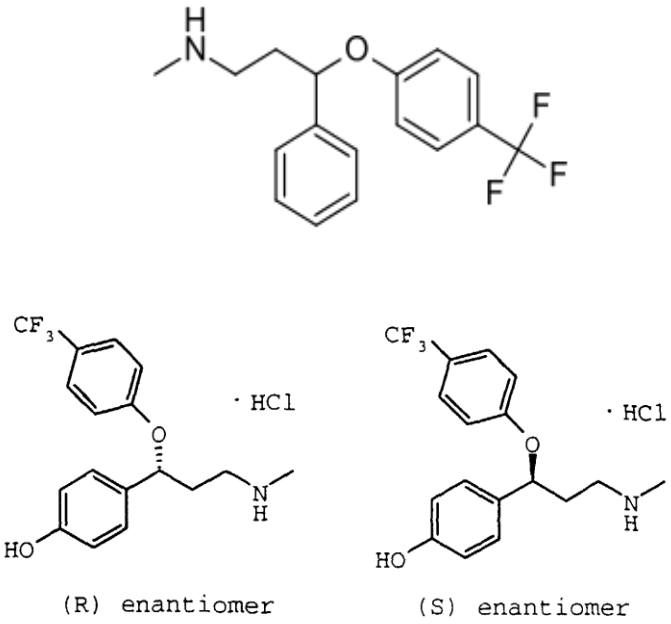

Figure 2 Structure of Fluoxetine and its R- and S-enantiomers

Simvastatin (brand name Zocor), is a statin which has also been shown to increase neurogenesis, as well as improve spatial learning in rat models after a traumatic brain injury [11-13]. Cui and colleagues found that simvastatin treatment increased synaptic plasticity and promoted neuro-blast migration in the sub-ventricular zone of the ischemic brain [14]. Figure 3 indicates the organic structure of Simvastatin.

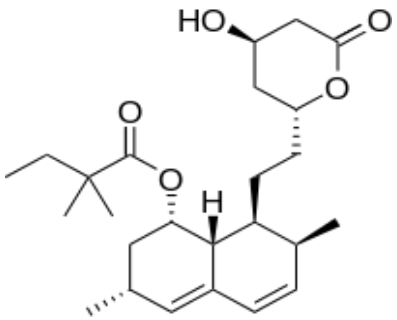

Figure 3 Structure of Simvastatin

In addition to these two potent drugs, *Corbett et. al* [9, 15] has combined ascorbic acid (vitamin C), fluoxetine, and simvastatin as a combination therapy for neurogenesis after stroke. Ascorbic acid is an antioxidant. It may therefore enhance the effects of fluoxetine by protecting the serotonin from oxidation. It may also protect endothelial nitric oxide synthase (*eNOS*) from oxidation, thereby enhancing the effects of simvastatin [9, 16]. Simvastatin exerts an anti-oxidative effect through inhibiting an increase in the levels of serum 8-isoprostane, a marker of oxidative stress in acute ischemic stroke patients. This could be partly due to ascorbic acid packed as an inactive ingredient in simvastatin and thereby implicitly contributes its anti-oxidative effects [17].

Another way that this combination may be beneficial to stroke patients is their combined effect on neurogenesis. *Corbett et. al* [9] indicates that simvastatin (0.5mg/kg) and ascorbic acid (20mg/kg) treatment in a daily dose did not produce any increase in neurogenesis, whereas the addition of fluoxetine (5mg/kg) produced nearly doubled neurogenesis over fluoxetine alone. The combination of fluoxetine/ascorbic acid treatment did not show any increase in functional recovery over fluoxetine alone, whereas the addition of simvastatin to the treatment showed a two-fold increase in functional recovery over fluoxetine alone. Overall, these studies indicate that drug treatment using the combination of 0.5mg/kg simvastatin, 5mg/kg fluoxetine, and 20mg/kg ascorbic acid can successfully increase neurogenesis, improve motor function, and increase plasticity of injured neurons. Thereby this also causes a smaller infarct after cortical, ischemic stroke in Long Evans female rat models [9].

The therapeutic potential of fluoxetine is implicated in the manifestations of different neurological disorders such as Alzheimer's disease, epilepsy, Huntington's

disease, and stroke [18]. For example, this antidepressant treatment also helps to achieve better recovery from disability after stroke onset [19]. A clinical study conducted in patients to investigate motor deficit after stroke, showed enhanced motor recovery after 3 months following a 20mg fluoxetine treatment compared to placebo [20]. This FLAME (acronym for – Fluoxetine for Motor Recovery After Acute Ischemic Stoke) clinical trial showed significantly greater Fugl-Meyer motor scale score at day 90 after adjustment for depression. In addition, a significant improvement in the modified Rankin scale evaluating independence in normal daily tasks was noted [21].

In humans, when compared to the control, antidepressants such as fluoxetine, has improved executive functions to maintain mental control and self-regulation, by modulating neuronal network associations involved with prefrontal functions (studied using magnetic resonance scans) and is attributed as a possibility to its neurotransmission and neurotropic activities [22]. A study from another laboratory indicates that the administration of fluoxetine for 7 days post stroke enhances motor function by maintaining synaptic plasticity through a reduction of inhibitory interneuron activity in the premotor cortex [23]. Fluoxetine has also been reported to produce neuro-blast cells in the sub-ventricular zone and the dentate gyrus of adult male Wistar rats a month after stroke induction [24]. However this study also found that oral administration of 16mg/kg/day of fluoxetine for 3 weeks (initiated 1 week after stroke) did not improve sensorimotor recovery and had no influence in the survival or differentiation of the newly generated cells possibly because this would translate into over 100mg dose in humans [24]. A pilot study indicated that fluoxetine influences motor output in chronic stroke patients by activating both agonist and antagonist muscles of the paretic arm, suggesting

that it may influence motor recovery [25]. Chronic fluoxetine treatment of 10mg/kg for 4 weeks improved spatial cognitive function recovery after ischemic stroke [26]. This drug has also been reported to improve cortico-cerebral blood flow after ischemic stroke in rabbits [27].

In nature, fluoxetine exists in a 50/50 racemic mixture of R-fluoxetine and S-fluoxetine enantiomers. The S-fluoxetine enantiomer is eliminated slowly and is present in the plasma at profound levels compared to the R-fluoxetine[28]. One study shows that the S-enantiomer is more potent compared to R-enantiomer in producing anorexic effects in meal-fed rats [29]. Fluoxetine is metabolized by the liver in its metabolite form called norfluoxetine, which is formed by demethylation of fluoxetine. Human liver enzyme cytochrome P450 (figure 4) has several isoforms that are largely involved in the metabolism of fluoxetine enantiomers [30]. In the process, R-/S-fluoxetine in the drug form is converted into metabolite forms such as R- or S-norfluoxetine, fluoxetine glucuronide, norfluoxetine glucuronide, and inactive metabolites. Cytochrome P2D6 is significant because it influences the formation of S-norfluoxetine, and cytochrome P2C9 is also significant as it influences the formation of R-norfluoxetine. In animal models, the activity of S-norfluoxetine is 20 times higher than R-norfluoxetine in SSRI potency and plasma concentrations of S-enantiomers are usually two times higher than R-enantiomers after several weeks of administration [30]. This is also demonstrated in a clinical study done in adult patients receiving 10 to 60 mg/d fluoxetine, in whom the plasma concentrations of S-enantiomers were higher than their R-enantiomers with a statistical significance of $P<0.0001$ [31].

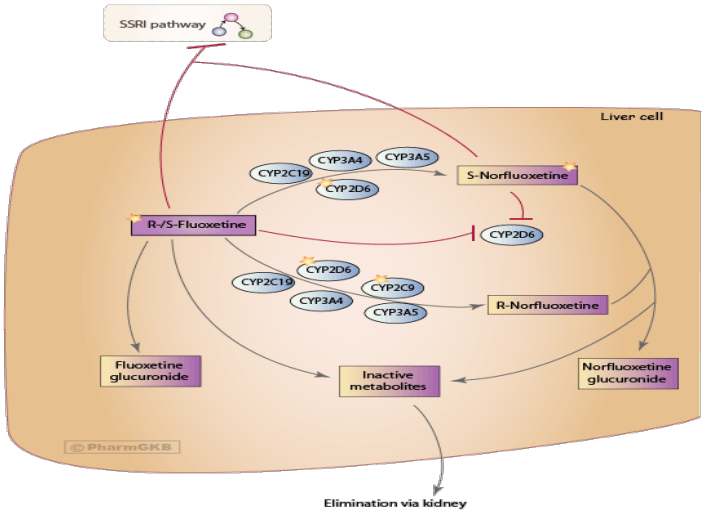

Figure 4 Enzymatic metabolism of fluoxetine. Fluoxetine enantiomers are metabolized to an active form called norfluoxetine by enzymes in a liver cell. Human liver enzyme cytochrome P450 has several isoforms involved in this process as shown. R-/S-Fluoxetine is the drug form metabolized into R- or S-Norfluoxetine, Fluoxetine glucuronide, Norfluoxetine glucuronide, and inactive metabolites via enzymatic action of indicated liver enzymes (blue circles). Starred enzymes are important and greatly influence the formation of a certain (R/S) metabolite enantiomer. Solid purple box indicates drug, shaded purple-yellow box indicates metabolite, yellow colored stars indicate significant, shaded blue oval bubbles represent specific liver enzymes (CYP – Cytochrome) [30]

Contradictory finding indicates at between 1 and 10 micro molar concentrations, R (-) enantiomer of fluoxetine is more effective than the S (+) enantiomer on neuronal channels and less effective on cardiac channels [32]. This epilepsy study found that R-fluoxetine had stronger anticonvulsant effects compared to S-fluoxetine in mouse models [32]. Also, increased serum levels of the active metabolite, norfluoxetine (which is an active form of S-enantiomer but, inactive for the R-enantiomer) at 112.66 ng/mL, is shown compared to fluoxetine levels at 19.285 ng/mL at 1-4 hours after ingestion [15]. The elimination half-life of metabolite form norfluoxetine is 7 to 15 days in humans, which is slow compared to the drug form fluoxetine elimination occurring quickly ranging from 1 to 4 days [33].

In this current project, several neuronal growth factor genes are believed to be influenced by fluoxetine enantiomers; I investigated both enantiomers which were up- or down-regulated and contribute to healing in the sub-ventricular zone after stroke.

Stroke Animal Models

Given the poignant statistics of stroke casualties in the United States of America, research on stroke requires a model that can closely resemble human biological characteristics and behavior. It is necessary to study stroke in an animal model that would yield results translational to human medicine. Since the 16th century, rats and mice are the most common laboratory animals used in biomedical research worldwide. They are financially cost effective and efficiently manageable to conduct experiments compared to other animals such as apes, which are occasionally used for single final experiment before clinical trials. Retired breeder Sprague Dawley rats were chosen as a model to study stroke recovery and neurogenesis in this project. The need to select retired breeder, aged models comes from the fact that the majority of stroke occurs in the elderly population. A Sprague Dawley rat is an outbred albino rat. This strain is most commonly used in neuroscience medical research as its brain anatomy and physiology is understood to be similar to that of humans.

Different stroke induction methods have previously been used to generate an average sized infarct. One study done in rats of 12-14 weeks' old used a modification of the MCAO method [34]. This method was modified to overcome problems associated with thread insertion into the narrow carotid canal of the middle cerebral artery (MCA) [34]. Improved stroke induction rates were noted by 14% to 86%. In addition, they showed decreased mortality from 21-31% to 3-7% after thread-occlusion of the middle

cerebral artery. During the procedure, the suture was retracted to reopen the MCA after injury [34]. An intraluminal suture method in the middle cerebral artery had only an 11% survival rate in mice, although this rate increased to 60% survival rate upon administering prophylactic antibiotics. This ischemia induction method resulted in severe functional impairment and loss of body weight [35].

There are two methods commonly used to induce a stroke in animal models. First method commonly used to produce stroke in rats is called a middle cerebral artery occlusion (MCAO). In a thromboembolic MCAO procedure, blood clots are directly injected into the carotid artery of the animal. In an endovascular filament MCAO procedure, a surgical filament is inserted in the carotid until it occludes the middle cerebral artery, which then results in blocked vascular flow hence producing an infarct. These MCAO procedures produce variable infarct sizes and are also only applicable to certain rat strains [36]. The transcranial MCAO procedure is a method which requires a craniotomy. This procedure involves surgical dissection of the middle cerebral artery and is then permanently occluded to produce focal ischemia [36]. Acoustic startle reflexes have been shown to be altered due to permanent middle cerebral artery occlusion after surgery in Sprague Dawley rats [37]. Reversible MCAO method using an intraluminal suture is a reliable and effective method in younger rats, but the size of the infarct produced is much larger than the size produced in humans. Generally older rats don't survive the stroke under this method. Therefore, we suggest that this method is not the best model to imitate human stroke. However, the MCAO suture can be removed, allowing for reperfusion injury in these animals [38]. Middle cerebral artery occlusion (MCAO) rodent models were not used in this study because it produces very large infarct

volumes, which again does not closely resemble the average sized human stroke infarct [39].

Focal ischemia is a second method in which reduced ischemic stroke induced either with a vasoconstrictor or photo-thrombosis in rats. A potent vasoconstrictor, endothelin-1, is injected near the middle cerebral artery to induce focal ischemia and stroke via constriction of arteries and veins. We chose this method in this project because of the low mortality rates (less than 10%) and the ability to produce reproducible infarcts in the forelimb motor cortex in aged rats [36]. In another focal ischemia method called distal MCAO, the middle cerebral artery is electro-coagulated on the surface of the brain, away from its origin in the circle of Willis. The stroke that is induced is similar in size of that occurring in humans, but the surgery is very difficult on older rats because of a risk of bleeding out of the artery [40].

Another focal ischemia method commonly used to produce stroke in rats involves photochemical occlusion of irradiated vessels. It is performed by intravenous injection of photosensitive dyes such as rose-bengal leading to photocoagulation of circumscribed cortical areas inside the brain via a small hole in the skull. This procedure is not used in our project because the photo-chemically induced blood clot might damage the endothelial Nitric Oxide Synthase (*eNOS*) present in the inner lining of the blood vessels in the sub-ventricular region and then it would be unable to respond to the statins. However, this method can use aged animals, produces small infarct in specific areas and demonstrates a high survival rate of 100% following surgery [41].

Stress and Neurogenesis

Stress has a profound effect on neurogenesis, which eventually leads to significant decrease in cell proliferation in the adult hippocampus region and in the sub-ventricular zone [42, 43]. One study performed *in vitro* showed anti-proliferative effects on cultured neural stem cells dissected from the sub-ventricular zone, due to high cortisol levels in the blood obtained before the animals were euthanized [44]. A research finding in Sprague Dawley rats showed reduced proliferation of cells affected in the sub-ventricular zone (figure 5) by chronic traumatic-brain injury, but the neuronal cell differentiation profile remained unaffected [45].

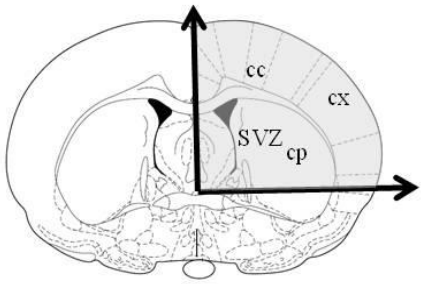

Figure 5 Schematic diagram of sub-ventricular zone of a rat brain. (SVZ: sub-ventricular zone, cc: corpus callosum, cx: cerebral cortex, cp: striatum-caudate putamen) [46]

Because neurogenesis is the subject of prime interest of this study, particularly after the induction of stroke which is considered traumatic, methods to keep the stress levels at a minimum were deemed necessary to prevent its effects on neurogenesis. A study suggested that rats injected intraperitoneally with hypertonic saline injections once daily for 14 days showed significantly increased corticosterone levels thereby resulting in chronic stress [47]. Therefore, in this present project we have used reliable voluntary oral administration of FDA approved drugs chosen to enhance neurogenesis [15]. This

method is proven to cause no stress because whether the animal will consume the drug is a voluntary decision. *Corbett et. al* [15] utilized fluoxetine to promote neurogenesis, which corresponds with the conclusions from *Warner-Schmidt et. al* [42] study that chronic antidepressant treatment up-regulates hippocampal neurogenesis, and could thereby block or reverse the damage caused due to stress. I propose the possibility that fluoxetine may up-regulate neurogenesis in the sub-ventricular zone in this study.

Gene Expression

Molecular and Cellular Effect on Neurogenesis

Neurogenesis is the process by which neurons are generated from neural stem cells or progenitor cells. The subject of neurogenesis is very intricate because it constitutes several pathways in its course of action during the period of regeneration. Although given its complexity, an insight into neurogenesis can be achieved through the study of gene expression, which is the process of transcribing genes into a functional gene product such as mRNA and proteins. This product can be analyzed to understand the pathways involved in leading to neurogenesis inside the brain, particularly after the post-stroke delayed drug treatment involved in this project. Table 1 describes the neurogenesis genes and their functions that we have chosen to study in this project.

Table 1 – Neurogenesis Gene markers and their functions

Bdnf	Maintenance of neurons; growth and differentiation of neural stem cells; learning and memory organization
Camk2a	Spatial learning; neurotransmitter release
Camk2g	Synaptic plasticity to govern spatial learning
Ccl11	Decreases neurogenesis with age; allergic responses
Cntf	Survival of neurons; reduces tissue destruction during inflammatory attacks
Cntfr	Neuronal cell survival and differentiation; signal transduction; gene expression
Creb1	Transcription factor
Crh	Neuroendocrine and behavioral responses to stress; cell growth and survival; synaptogenesis; circuit integration of adult-born neurons
Nos2	Neurotransmission
Plat2	Tissue remodeling; cell migration; breakdown of blood clots
Vegfa	Vascular permeability; apoptosis inhibition

An FDA approved SSRI drug, fluoxetine has been shown to up-regulate genes associated with brain-derived neurotropic factor (*Bdnf*) which induces long term potentiation (LTP) [48]. This leads to the fact that tracing genes involving the *Bdnf* could lead to potential pathways of neurogenesis. Another such study provides evidence that fluoxetine treatment leads to increased gene expression levels of mRNA for glucose transporters namely GLUT1 and GLUT10 [49]. These glucose transporters play key roles in homeostatic control of brain functions.

Similarly, administration of simvastatin has been shown to alter multiple gene expression patterns in the cerebral cortex [50]. *Chen et al*. [16] indicates a role for statins in increasing *Bdnf*, which would aid in neurogenesis as mentioned earlier. Administration

of the statins is very beneficial for the treatment of stroke because it induces not only neurogenesis, but also angiogenesis and synaptogenesis thereby enhancing the functional outcome [51].

A growth factor, called insulin-like growth factor 2 (*IGF2*) is shown to be selectively controlling the proliferation of dentate gyrus neural stem cells *in vitro* and *in vivo* through AKT-dependent (AKT stands for Protein kinase B) signaling, thus proving that *IGF2* is a novel regulator of adult neurogenesis [52]. Also in the sub-ventricular zone, endothelial-derived *IGF2* is implicated in maintaining neural stem cells [53].

Certain brain resident immune cells have also proven their contribution to the regeneration of neurons. Microglia are found in the forebrain region of sub-ventricular zone (SVZ) of the rat, where neurogenesis is enhanced via the release of cytokines [54]. In addition to neurogenesis, microglia are predominantly known for causing inflammation and oxidative stress inside the brain.

We believe that studying gene expression changes associated with post-stroke fluoxetine, simvastatin, and ascorbic acid combination drug treatments on neurogenesis could elucidate further pathways involved in brain recovery. This research may aid further studies which can help discover better stroke treatments.

Fluoxetine and Simvastatin Influencing Polarization of Microglial Subtypes

Stroke causes neurological damage as a result of blockage of normal blood flow. This occlusion undoubtedly provokes a physiological mechanism to fight the disturbance and correct it back using homeostasis. The immune system is one such mechanism that is activated instantly triggering the release of cytokines and chemokines.

Microglia are resident macrophages of the brain that play a role in attacking foreign substances entering the central nervous system and in inducing neuro-inflammation. The brain is protected by a physical barrier called the blood-brain barrier (BBB), which is made up of endothelial cells that exclude certain foreign pathogens from crossing into the brain. This blood-brain barrier is a site of action for microglia, where its function is affected in certain neurological diseases such as ischemic stroke, epilepsy, multiple sclerosis, and Alzheimer's disease [55].

Evans Blue is a dye used to study vascular permeability in animal models. Evans Blue leakage into the brain parenchyma means that the blood brain barrier is disrupted [56]. This study reveals that spectroscopic measurement of this dye can be found in rat tissue samples, and quantities can be determined by standard curves established by mixing the dye with trichloroacetic acid [56].

Activated microglia can disrupt the blood-brain barrier and cause neurological damage in ischemic stroke. The cellular damage is caused by its production of reactive oxygen species (ROS) and nitric oxide (NO). Blood flow occlusion recruits microglial cells which release ROS such as NADPH (nicotinamide adenine dinucleotide phosphate hydrogen) oxidase, in addition to certain cytokines such as interleukin-6 (*Il-6*), interleukin-1beta (*Il-1β*), insulin-like growth factor-1 (*IGF-1*), and tumor necrosis factor alpha (*Tnf-α*), and certain chemokines such as *CXCL-1* [55]. The release of ROS and certain cytokines affects BBB permeability, thereby aggravating stroke. *da Fonseca et. al* [55] reports that the *Il-1beta* and *Tnf-alpha* down-regulate the tight junctions, and together with *Il-6* affect the expression of adhesion molecules of BBB endothelial cells. However, intracerebroventricular injection of microglia has been shown to protect BBB

permeability and neurodegeneration caused by ischemic stroke [57]. These contradictory findings suggest that microglia are implicated in neuro-inflammatory regulation at the blood-brain barrier and the gene expression of its cytokines will provide an insight into possible pathways of its action to understand its role in ischemic stroke.

Microglia provide innate inflammatory immunity to protect the brain. Macrophages exist in two distinct phenotypes according to their functionality. One group is classically activated and is pro-inflammatory. They are often referred to as type I, or M1. The other is alternatively activated and is anti-inflammatory. They are referred to as type II, or M2. The latter subset (M2) can be subdivided: M2a are involved in tissue repair, M2b are involved in B cell immunoglobulin-G production, and M2c are implicated in anti-inflammatory or scavenging mechanisms [58, 59]. These macrophage subtypes were originally studied in the peripheral macrophages, therefore the gene markers may or may not be associated with the microglia [58]. Some macrophage gene markers are present in microglia and some are not.

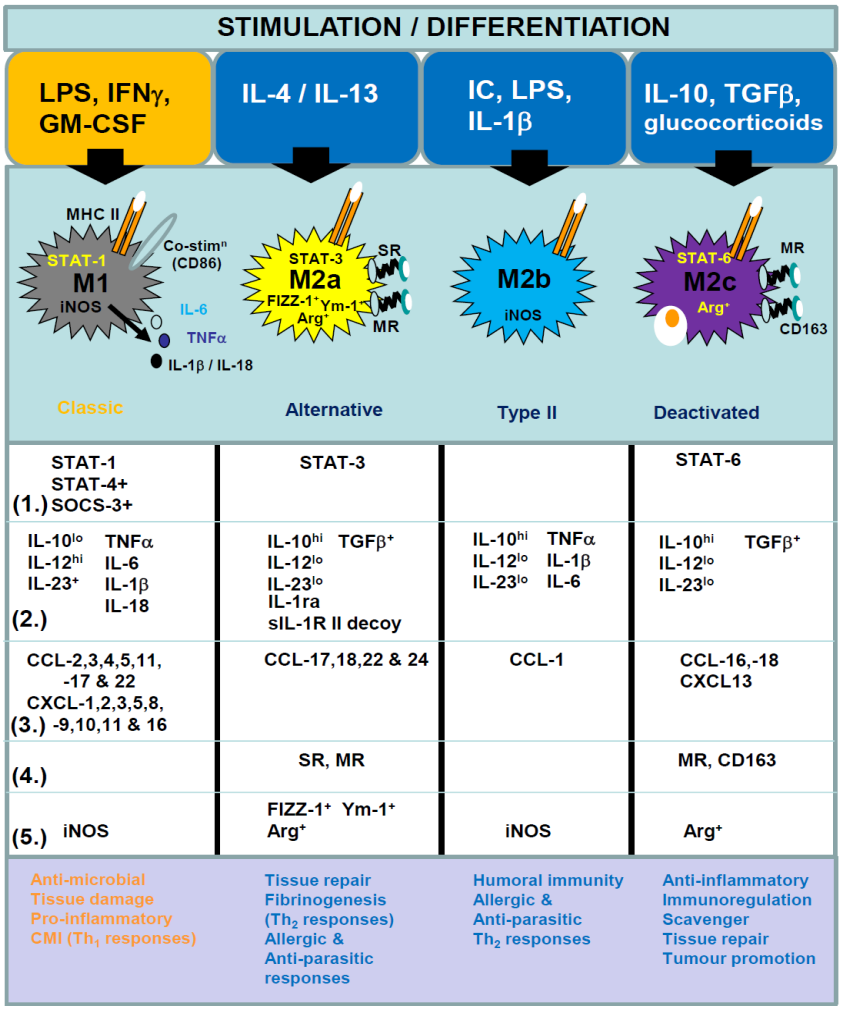

Figure 6 Gene markers involved in the stimulation and differentiation of macrophage subtypes M1, M2a, M2b, and M2c. M1 is classically activated and is pro-inflammatory. M2 is alternatively activated and is anti-inflammatory. The molecular markers listed in the table are categorized into functional phenotypes of (1.) signaling molecules, (2.) cytokine expression profile, (3.) chemokine profile, (4.) scavenger receptor expression, (5.) tryptophan metabolism. Lower segment summarizes the function of each subtype as M1 – anti-microbial, M2a – involved in tissue repair, M2b – involved in B-cell IgG production, and M2c – anti-inflammatory or scavenging mechanisms. Abbreviations: lipopolysaccharide (LPS), interferon gamma (IFNγ), interleukin-4 (IL-4), tumor growth factor beta (TGFβ), major histocompatibility complex II (MHC II), inducible nitric oxide synthase (iNOS), tumor necrosis factor alpha (TNFα), arginase (Arg), chemokine ligands (CCL-2, CXCL-1), cluster of differentiation 163 (CD163), and poorly defined effector molecules (FIZZ-1, Ym-1) [58]

Macrophages express a pool of cytokines and chemokines upon activation as shown in figure 6. Out of these we chose certain markers to study microglial gene

expression as listed in table 2. The gene markers of M1 studied in our project include *Tnf-alpha*, *Il-1beta*, and *Il-6*. Similarly, the gene markers of M1 that we focused on this study are *Ccl11* and *Cxcr-4* [58, 59]. Interleukin-10 (*Il-10*) is also an cytokine to identify M1 type, and a transcription factor called *Stat1* is believed to cause its polarization [58, 59]. Further research shows that the activation of *Stat1* inhibits *Stat6*, which is the transcription factor involved in M2 subtype polarization. Thereby, this finding suggests that the M1 polarization cross-regulates the M2 polarization; meaning that the activation of one suppresses the other and vice versa [58, 59]. In addition to *Stat6* transcription factor, *Il-10* and *Tgf-beta* are also studied to provide insight into M2 type activation. Arginase-1 is also a tryptophan-metabolism marker that is known to induce M2 polarization activity [58, 59]. Inducible nitric oxide synthase (*iNOS*) requires arginine to produce nitric oxide. If the enzyme arginase is present, it would break down the substrate that the *iNOS* needs, so it would directly work against the production of nitric oxide.

Table -2 Microglial Subtype Markers Used in this Study

M1 (Pro-inflammatory)	M2a (Anti-inflammatory)	M2b (Anti-inflammatory)	M2c (Anti-inflammatory)
Stat1	*Stat3*	*Il-10*	*Stat6*
Stat4	*Il-10*	*Tnf-alpha*	*Cd163*
Tnf-alpha	*Tgf-beta*	*Il-1beta*	*Il-10*
Il-6	*Arg1*	*Il-6*	*Tgf-beta*
Il-1beta		*Nos2*	*Arg1*
Ccl11			
Nos2			

Macrophage plasticity is governed by the switching of M1 pro-inflammatory to M2 anti-inflammatory macrophage or vice versa by the release of certain cytokines as mentioned earlier. It has also been discovered that the energy expenditure-associated with oxidative stress leads to conversion of M1 type to M2 type in the brain. The M1 type is pro-inflammatory activation of macrophages while the M2 type is understood to be an anti-inflammatory signaling and wound healing macrophages [60]. However, following a traumatic brain injury, one study showed that microglia simultaneously express both M1 and M2 phenotypes because of mixed signaling surrounding them inside the brain [61]. The pro-inflammatory M1 phenotype is expressed at the end stage of neurodegenerative diseases, which results in neuronal loss, therefore, studying a stage-specific switch of M1 to M2 type has been suggested to offer insight into therapeutic time window for better treatment [62, 63].

SSRIs have been implicated in modulating the immune system. Fluoxetine has been shown to down-regulate the activation of M1 pro-inflammatory microglia, and up-regulate the activation of M2 anti-inflammatory microglia [64]. Similarly, *Lim et. al* showed 10mg/kg of fluoxetine administered intravenously after stroke induction by MCAO caused suppression of the pro-inflammatory marker NF-kappaB [65]. Fluoxetine has also been shown to inhibit lipopolysaccharide(LPS)-induced microglia activation, certain pro-inflammatory cytokines, and toxic factors including *Tnf-alpha*, *Il-1beta*, and nitric oxide [66, 67]. Another study published in 2015 showed fluoxetine inhibited the activation of microglia after spinal cord injury and protected oligodendrocytes from cell death [68]. Also, fluoxetine treatment down-regulated microglia activation in neuropathic pain [69]. Administration of aspirin (acetylsalicyclic acid) enhanced the anti-inflammatory effect of fluoxetine by inhibiting the LPS-induced activation of pro-inflammatory microglia and promoting that of anti-inflammatory microglia [70]. SSRIs, including fluoxetine inhibited microglial *Tnf-alpha* and nitric oxide production, along with cAMP signaling [71]. Microglia in the brain are seen to be activated by interleukin-1beta (*Il-1b*), which in turn increased significantly upon administration of fluoxetine [72].

Similarly, simvastatin treatment alters the release of cytokines and trophic factors in a cholesterol-dependent manner. Upon administration, it also inhibited phagocytosis in microglia in a cholesterol-independent manner [73]. Also, administration of simvastatin has been proven to attenuate microglial activity to produce anti-inflammatory responses after ischemic stroke by releasing cytokines such as *Il1-beta*, *Tnf-alpha*, and *Bdnf in vitro* [73].

There is interesting evidence in mice after injection of *Il-4* showing that microglia are responsive in a temporal-spatial fashion [74]. The ability of microglia to respond to neuro-inflammation ultimately depends on the number of microglial cells activated and their polarization. Local cytokines and cellular environment has been implicated in playing a role in causing their stimulatory activity [74].

In addition to cytokines such as *Il-6*, *Il-1β*, *Igf-1*, and *Tnfα*, microglia are implicated in up-regulation of *Stat1* transcription factor in response to cerebral ischemia [75]. Likewise, *p-Stat3* is also highly expressed after cerebral ischemia in mice and is believed to play a role in neuronal cell death [76]. Interleukin-6 (*Il-6*) has a direct effect on microglial activation of *Stat3* and this particular transcription factor plays a role in long-term recovery after stroke [77, 78]. Manwani and colleagues found that biological sex has a differential effect on the inflammatory response post-stroke, showing that female rats display increased level of expression of anti-inflammatory microglia compared to male rats [79]. Age is another factor that enhances neuronal degeneration, alters microglial response with increased pro-inflammatory cytokine expression, and also changes the time-course of activation of *Stat3* transcription factor [80].

II. MATERIALS AND METHODS

Sprague Dawley rats were received from Harlan, and housed in the Laboratory Animal Care facility. Each rat was housed in an enclosed shoe-box sized cage separately, at the room temperature of nearly 74 degrees Fahrenheit. They were fed with a Harlan rat chow, restricted at times during the course of the experiment for the purpose of motor functional tests. The restricted diet was weighed at 85% of the ad lib food, ranging from 9.6 grams to 12.4 grams, with an average of 10.2 grams.

Montoya Staircase

Figure 7 Montoya Staircase. Sprague Dawley rat in a Montoya Staircase apparatus to test bilateral forepaw motor functioning.

Sprague Dawley rats participated in Montoya staircase training for the purpose of motor functional analysis. The Montoya staircase apparatus is an enclosed rectangular box with the dimensions of 10 by 12 inches (see figure 7). It consists of seven steps on each side separated by a platform to test front left and front right forepaw motor function. Each step has a depression which was filled with three Bio-Serv 45-mg Chocolate Flavor Dustless Precision Sucrose Pellets. The rats were transported and kept inside the apparatus for 15 minutes. This training was carried out in a dark phase.

The rats were fasted during the day with restricted diet administered only after the training. The fasting condition induced them to consume sucrose pellets voluntarily immediately when placed inside the apparatus. At the end of training, both sides of the staircase were checked to record the number of pellets consumed using each left and right paw. This training was performed before and after endothelin-induced stroke surgery to record the numbers of pellets each rat consumed and to perform the motor functional analysis. Our baseline criteria were that each rat must learn to retrieve at least 9 pellets with the left paw in order to be included in later functional tests. The average number of pellets retrieved was generally 15-18 for each paw.

For the purpose of functional analysis, data from training conducted the final three days' pre-stroke and post-stroke surgery (3-day trial period: post-stroke days 3, 4, 5) were selected. Of those three day trials, one best performance (highest total number of pellets retrieved overall) was chosen to calculate contralateral and ipsilateral functional deficit. The mathematical formula used to calculate contralateral function after stroke was dividing the number of pellets retrieved by the left paw post-stroke by the number of pellets retrieved by the left paw pre-stroke. If the post-stroke performance is the same as

the pre-stroke performance, the ratio would be one. If the post-stroke performance is less than the pre-stroke performance, then the contralateral performance would be somewhere between 0 and 1. Similarly, the formula used to calculate ipsilateral function after stroke was dividing the number of pellets retrieved by the right paw post-stroke by the number of pellets retrieved by the right paw pre-stroke.

Endothelin-Induced Stroke Surgery

The following day of completion of Montoya training, surgery was performed to induce stroke for the purpose of the study. Eight rats assigned to a group, with a total of three groups, were scheduled for the surgery each day. The purpose of assigning surgical groups (different from the treatment groups) was to ensure that each rat had followed Montoya tests and drug treatment on the same post-stroke days, because completion of all surgeries in a single day was physically unfeasible. Prior to the start of surgery, the rats were placed into an induction chamber boxed with oxygen running at 0.6 liters per minute and isoflurane at 5% for a total of 4 minutes. When the animal was under the plane of anesthesia, the top of the head was shaved using an electronic shaver starting at slightly above the eyes to past the ears medially. The rats were mounted into a stereotactic apparatus using non-traumatic ear bars and fitted with an anesthesia mask with 2% isoflurane flowing continuously. Eye lube was administered to both eyes to keep them lubricated during the surgery. The shaved area was scrubbed with provoiodine, then 70% ethanol, then again, a final scrub of provoiodine, which was left in place. Next, a slit was made midway between ears with a pair of scissors extending from just above eyes till a short distance in front of ears, and then bupivacaine was dropped onto the edges of the incision. Anatomical position called bregma was located and marked with a permanent

marker pen. A hand held drill with a burr drill bit was mounted into the stereotactic apparatus and the drill bit was aligned to bregma, and the stereotactic coordinates of bregma were recorded. We then moved 2.5 millimeters lateral (to the right side), where the first hole was drilled. From this position, we then moved 1.5 millimeter anterior, where the second hole was drilled. Sterile endothelin (reconstituted in acetic acid and water at a concentration of 400 pmoles/microliter) was kept in an ice bath, then taken up into a Hamilton syringe (3 microliters total) and then 1.5 microliters (600 pico-moles) was injected into each of the two holes at a depth of 2 millimeters, adding only 0.1 microliters every 10 seconds. The slit was sutured up to close using discontinuous stitches. When rats regained consciousness, they were transferred to a warm bed and kept there for post-surgical recovery for 15 minutes, after which they were transferred to their individual cages. They were allowed to consume *ad lib* moist chow on the day of surgery.

Voluntary Drug Administration

Sprague Dawley rats were administered the FDA approved drugs of 5mg/kg Fluoxetine (manufactured by Lilly), 1mg/kg Simvastatin (manufactured by Northstar RX), and 20mg/kg Ascorbic Acid (manufactured by Sigma-Aldrich). Table 3 shows the drugs administered to animal groups and lists the abbreviations used for each group in the results and discussion sections of this project.

GROUPS	ABBREVIATIONS	DRUGS
Female Control Group	FC	No drugs
Female FSA Group	FFSA	Fluoxetine Simvastatin Ascorbic Acid
Female S-Fluoxetine Group	FS-Flu	S-Fluoxetine Simvastatin Ascorbic Acid
Female R-Fluoxetine Group	FR-Flu	R-Fluoxetine Simvastatin Ascorbic Acid
Male S-Fluoxetine Group	MS-Flu	S-Fluoxetine Simvastatin Ascorbic Acid
Male R-Fluoxetine Group	MR-Flu	R-Fluoxetine Simvastatin Ascorbic Acid

Table 3 Drugs administered to the animal groups and a list of the abbreviations used for each group in the following sections of this project. Drugs were administered in fixed dosages as 5 mg/kg fluoxetine, 1 mg/kg simvastatin, and 20 mg/kg ascorbic acid.

Each rat was given the drugs weighed and rolled into a Pillsbury brand sugar cookie dough 4-gram rolled rounds. Each of the three drugs were weighed according to the body weight index and mixed together with over-night refrigerated and weighted cookie dough. All drugs were placed into a central indent into the dough, which was

made using a finger, and then rolled into rounds to completely encase the drugs. They were then placed into plastic boats which were placed inside animal cages for consumption. Control animals received plain Pillsbury sugar cookie dough rounds with no drugs. This procedure was performed at the same time in the afternoon each day, beginning 20-26 hours after stroke induction.

Euthanization and Cardioperfusion

Each Sprague Dawley rat was euthanized through intraperitoneal injection containing pentobarbital (Euthasol). When the animal was under a surgical plane of anesthesia, they were injected with a one milliliter Evans Blue dye directly into the ventricles of the heart. Next, they were cardio-perfused using a phosphate-buffered saline injection. Consecutively, the brain was dissected, and then quickly frozen in dry ice with isopentane.

Cryostat

Dissected brains from Sprague Dawley rats were kept frozen for three days in a deep freezer at -86 degree Celsius. Except the duration of the cryostat procedure, they were kept on dry ice when not in the freezer. First, each brain was glued onto the block using Tissue Tek O.C.T. Compound. Next, the brain was carefully sliced until the area of the infarct was detected in the right hemisphere. Sections were cut out using fine forceps in a chunk containing the infarct on the right hemisphere. Constant temperature of -30 degree Celsius was maintained throughout the procedure.

Real-time Polymerase Chain Reaction Gene Array

To investigate the genes involved in neurogenesis, a Qiagen real-time profiler PCR mini array kit was used. A 96-well custom plate was designed and utilized to amplify the genes of interest as shown in figure 8.

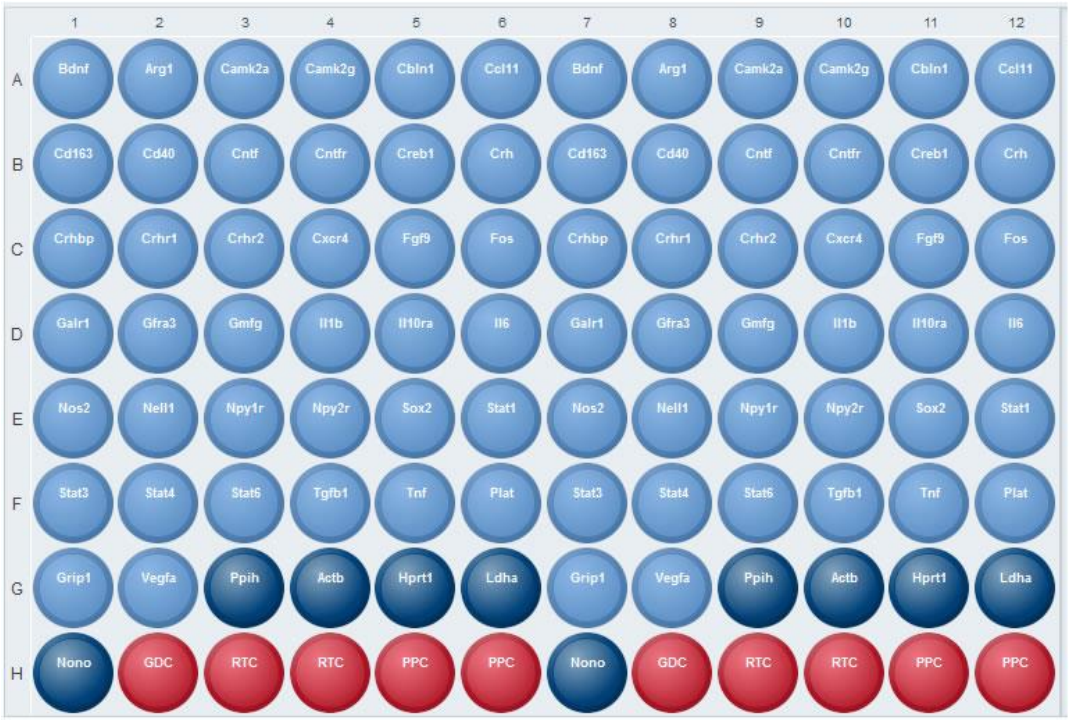

Figure 8 PCR Gene Array 96-well Custom Plate. Each gene has a duplicate. (Light blue wells – genes of interest, dark blue wells – housekeeping genes, red wells – control wells). Control wells include GDC – genomic DNA contamination, RTC – reverse transcription control, and PPC – positive PCR control.

Construction of mRNA after tissue homogenization: Each sample was first weighed to obtain between 20 to 30 milligrams of the tissue. This was calculated by subtracting the weight of an empty vial from the weight of the vial plus tissue. Then, 600 microliters of Qiagen RNeasy RLT Plus lysis buffer were added to the tissue in the vial and washed down to the bottom of the vial using the pipette. This tissue was completely lysed using a Tissue Tearor – Model 985-370 Type 2 at about 2,000 rpm, to obtain a homogenized lysate. Next, this lysate was centrifuged at maximum speed of 16,000 x g for 3 minutes.

Using a pipette, the supernatant was removed and placed into a Qiagen gDNA Eliminator mini spin column inside a 2 ml collection tube. The tube was centrifuged at 8,000 x g for 30 seconds. The flow-through volume was saved while the column was discarded. Then, 600 microliters of 70% ethanol were added to the flow-through and mixed well by pipetting up and down. 700 microliters of the sample and any remaining precipitate was transferred into a Qiagen RNeasy spin column inside a 2 ml collection tube. This mixture was centrifuged at 8,000 x g for 30 seconds and repeated once again after discarding the flow through volume. Next, 700 microliters of Qiagen RW1 (RNA Wash 1) wash buffer was added to the RNeasy spin column and centrifuged at 8,000 x g for 30 seconds. The flow-through volume was discarded. Then, 500 microliters of Qiagen RPE (RNA Pre-Eluant) wash buffer was added to the RNeasy spin column and centrifuged at 8,000 x g for 30 seconds. Again, the flow-through volume was discarded. Then, again 500 microliters of Qiagen RPE wash buffer was added to RNeasy spin column and centrifuged at 8,000 x g for 2 minutes. The spin column was placed into a 2 ml collection tube and centrifuged at 16,000 x g for 1 minute to further dry the membrane. Now, the RNeasy spin column was placed into a 1.5 ml collection tube. Next, 40 microliters of RNase-free water were pipetted into the spin column and centrifuged at 8,000 x g for 1 minute to elute the RNA. This step was again repeated after adding 20 microliters of RNase-free water to the spin column. The mRNA was stored in a deep freezer at -80 degrees Celsius.

Prior to its storage in a freezer, the concentration of mRNA was measured using a NanoDrop Spectrophotometer instrument. A drop containing one microliter of the sample was carefully placed on the NanoDrop, which yielded a graph along with concentration in

ng/μL and the salt-contamination in the sample. This step was repeated twice to obtain the average of the concentration.

Synthesis of cDNA from mRNA: Frozen messenger RNA stored in vials were first thawed to obtain the contents into a liquid form. Next, calculated amounts of mRNA, RNase-free water, and buffer Genomic Eliminator (Qiagen brand) were mixed into a vial using a 10 microliter pipette. Calculations were figured as not to exceed the volume of 10 microliters total in the vial. Contents were mixed and brought to the bottom of the vial using a centrifuge. Next, this genomic DNA elimination mix was incubated at 42 degrees Celsius for 5 minutes and then immediately placed onto ice for at least 1 minute.

Total volume of ten microliters of reverse-transcription mix was prepared by mixing 4 microliters of 5x Buffer BC3, 1 microliter of Control P2 (Primer and external control mix), 2 microliters of RE3 Reverse-Transcription Mix, and 3 microliters of RNase-free water. This RT mixture was added to each vial containing 10 microliters of genomic DNA elimination mix, and then mixed gently via pipetting up and down. Again, this mixture was incubated at 42 degrees Celsius for exactly 15 minutes and then immediately at 95 degrees Celsius for 5 minutes. Last, 91 microliters of RNase-free water was added and mixed by pipetting up and down, and then stored in a freezer at -20 degrees Celsius.

Real-time Polymerase Chain Reaction:

First, RT-PCR Components Mix was prepared in a 5 ml tray using a pipette. In order to prepare this mixture, Qiagen RNase-free water was added to the tray in two parts: 700 microliters, followed by 600 microliters using a pipette to make a total of 1300 microliters. Then, 1350 microliters of Qiagen 2x RT^2 SYBR Green Mastermix was added

after centrifuging, and mixed by pipetting up and down. Next, 102 microliters of thawed cDNA synthesis reaction were added and again mixed by pipetting up and down. This mixture was transferred into a 96-well plate using an 8-channel pipette delivering 25 microliters in each well. The plate was centrifuged at 1000 rpm for 2 minutes and repeated until absence of air bubbles was ensured. Thus prepared 96-well plate was inserted into a RT-PCR software instrument to obtain data for analysis.

The data obtained from the software was transferred into an Excel document, which was then uploaded to Qiagen website for RT-PCR data analysis. The volcano plots generated by the website were enhanced using Adobe Photoshop for labeling and coloring of the gene markers.

Evans Blue Spectrophotometer

Tissue containing Evans-blue dye was dissected in chunks from the cerebral cortex and cerebellum of the rat brain samples. Each tissue was weighed and collected into separate vials, to which the calibrated trichloroacetic acid (TCA) solution was added. The solution was prepared in a 1:4 ratios by mixing 100 microliters of artificial cerebrospinal fluid (ACSF) in 400 microliters of 50% trichloroacetic acid (TCA). The tissue samples submerged in the calibrated solution was homogenized using a Tissue Tearor – Model 985-370 Type 2. Next, the samples were centrifuged at 10,000 rpm for 20 minutes. Supernatant was separated and retained from the pellet using a pipet.

Next, 30 microliters of supernatant were added to the clear 96-well plates in three replicates. Then, 90 microliters of 95% ethanol were added to each well. The plates were run in a spectrophotometer instrument which yielded fluorescence values excited at 620nm and emitted at 680nm. These values are used for linear regression analysis to

obtain micrograms per gram of each tissue fluorescing Evans Blue, which are plotted using a GraphPad Prism software.

Statistical Analysis

One-way Analysis of Variance (ANOVA) was used to determine the statistical significance among different groups of female and male rats. The P-value < 0.05 is considered significant. Unpaired t-test with Welch's correction was used to compare statistics between two groups at a time. GraphPad Prism6 was utilized to generate the graphs in this project.

III. RESULTS

Montoya Staircase Motor Functional Analysis

The Montoya Staircase motor functional data was obtained from the last 3 days of pre-stroke training and animals were retested on post-stroke days 3, 4, and 5. Both right and left paw function was recorded as the number of sucrose pellets retrieved by the rats on each of those days. Data from the day with most number of pellets retrieved was chosen for the analysis. We did not take the average of the 3 days because we wanted to study the best performance within those three days for both right and left paw.

GROUP	# OF RATS	EXCLUSIONS (# OF ANIMALS)	REACHED TRAINING CRITERIA	CONTRALATERAL DEFICIT REACHED ≥ 20%	IPSILATERAL DEFICIT REACHED ≥ 20%
FC	6	1*	6*	5	2
FFSA	6	1©	6	5	1
FS-flu	6	1# , 1*	5*	5	2
FR-flu	6	2#	4	4	2
MS-flu	6	1§ , 1Ш	5	4	4
MR-flu	6	1§ , 2©	5	3	1

Table 4 Montoya Staircase Functional Data Table. In order for animals to reach the training criteria and thereby become included in this part of study, they had to pick up at least 9 pellets with either right or left paw. Deficit of greater than or equal to 20% was also a requirement to qualify for this part of study. Exclusions column indicates animals that were excluded in this part of study for reasons marked by symbols: § indicates did not survive post-surgery; # indicates animal retrieved no pellets pre-stroke; * indicates animal obtained ≥9 pellets with left paw, this animal is excluded in ipsilateral deficit but included in contralateral deficit, © indicates animal did not reach at least 20% deficit on both sides, Ш indicates animal excluded in contralateral deficit but included in ipsilateral deficit. (FC - Female Control, FFSA - Female Fluoxetine, Simvastatin, Ascorbic Acid, FS-flu – Female S-Fluoxetine, FR-flu – Female R-Fluoxetine, MS-flu – Male S-Fluoxetine, MR-flu – Male R-Fluoxetine)

Table 4 above shows exclusions and criteria used in the Montoya staircase test. A functional deficit of greater than or equal to 20% is necessary for the post-stroke analysis criteria and thereby only those animals are included in this part of study. With stroke induced on their right hemisphere, animals who retrieved greater than or equal to nine pellets with left paw were also included, however animals that retrieved no pellets on pre-stroke days were excluded from the study. Also excluded were animals that died post - surgery.

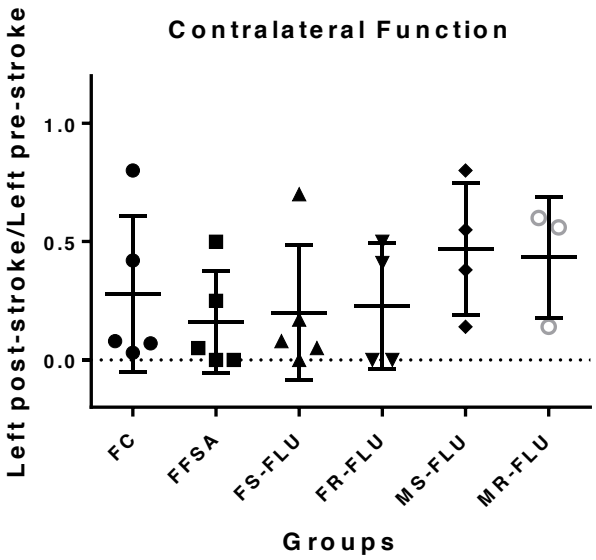

Figure 9 Graph showing the paw contralateral function, with each data point representing an individual animal and it is plotted with a wide horizontal bar which represents a group mean with standard deviation error bars. (FC - Female Control, FFSA - Female Fluoxetine, Simvastatin, Ascorbic Acid, FS-flu – Female S-Fluoxetine, FR-flu – Female R-Fluoxetine, MS-flu – Male S-Fluoxetine, MR-flu – Male R-Fluoxetine)

The paw contralateral function is obtained as left post-stroke number of pellets retrieved divided by left pre-stroke number of pellets. The contralateral function is plotted in figure 9 using the group mean with the standard deviation error bars. There are

no statistically significant differences among the mean values, with the *P*-value equal to 0.5272, derived using the one-way Analysis of Variance (ANOVA) statistical analysis. A contralateral function of 1 would mean that the animal has the same baseline function with that paw post- and pre-stroke, which would also mean that there was no functional deficit from the surgery, and therefore such an animal would be excluded from this part of study. However, if an animal picked up 8 pellets with its left paw after stroke compared to 10 pellets pre-stroke, then it retained 80% contralateral baseline function of its pre-stroke performance, and the contralateral function value on the graph would be at 0.8 on the y-axis.

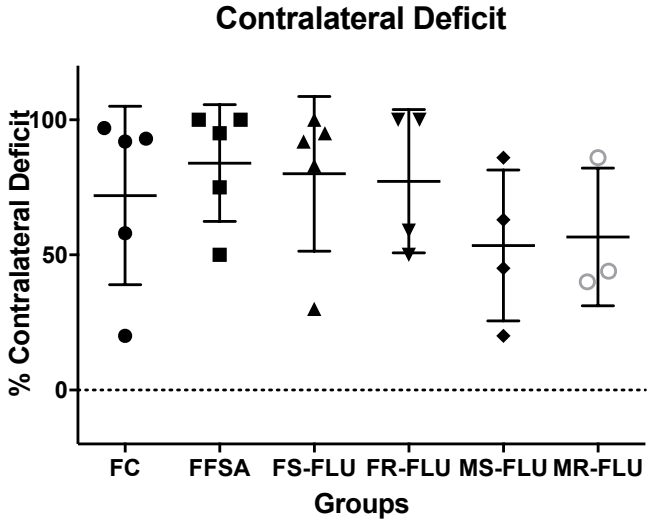

Figure 10 Graph showing the percent paw contralateral deficit, with each data point representing an individual animal and it is plotted with a wide horizontal bar which represents a group mean with standard deviation error bars. (FC - Female Control, FFSA - Female Fluoxetine, Simvastatin, Ascorbic Acid, FS-flu – Female S-Fluoxetine, FR-flu – Female R-Fluoxetine, MS-flu – Male S-Fluoxetine, MR-flu – Male R-Fluoxetine)

The paw contralateral deficit is a normalized value obtained by subtracting contralateral function value from 1. Both values complement each other in such a way that a 90% contralateral deficit post-stroke indicates a 10% baseline contralateral function

post-stroke compared to its pre-stroke function. For example, if an animal picked up 10 pellets with its left paw before stroke and 6 pellets after stroke with that same paw, then the contralateral baseline function was 60% of the pre-stroke function, with a 40% deficit on the left paw. Consequently, if an animal retrieved 15 pellets with its left paw pre-stroke and 12 pellets with left paw post-stroke with a 20% deficit in the left paw, then this translates as 80% contralateral baseline function. Figure 10 shows the contralateral deficit passing the 20% threshold deficit criteria across all groups and is graphed as a group mean with standard deviation error bars. Differences among the mean values are not statistically significant, and the *P*-value was 0.5340 obtained using one-way ANOVA statistical analysis.

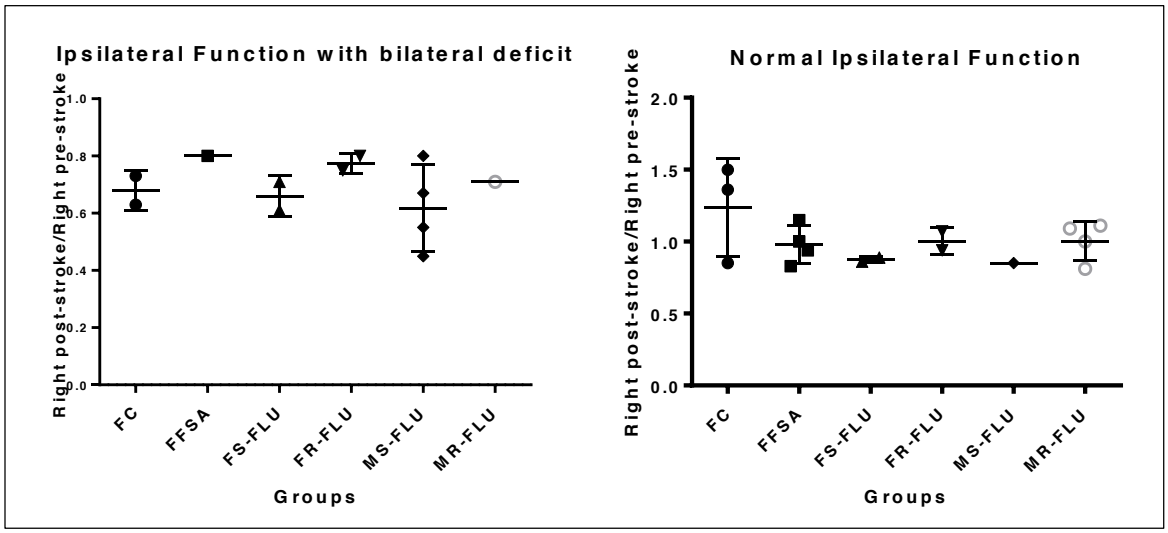

Figure 11 Graphs showing the paw ipsilateral function. The left panel of the graph shows ipsilateral function with bilateral deficit, and the right panel of the graph shows ipsilateral function with only ipsilateral deficit of less than 20% labeled as normal. Each data point on the graph is representing an individual animal and it is plotted with a wide horizontal bar which represents a group mean with standard deviation error bars. (FC - Female Control, FFSA - Female Fluoxetine, Simvastatin, Ascorbic Acid, FS-flu – Female S-Fluoxetine, FR-flu – Female R-Fluoxetine, MS-flu – Male S-Fluoxetine, MR-flu – Male R-Fluoxetine)

The paw ipsilateral function as plotted in figure 11 was obtained as dividing right post-stroke number of pellets retrieved by right pre-stroke number of pellets retrieved.

Only the animals reaching 20% bilateral deficit on both sides (right and left) are included in the left panel of figure 11, to determine any impaired function of the right paw. The right panel of figure 11 includes animals with less than 20% ipsilateral deficit in the right paw, to determine their normal baseline ipsilateral function for an animal that had a unilateral stroke. The values are plotted as a group mean with standard deviation error bars. One-way ANOVA analysis could not be performed because it requires each group to have at least two or more data points, and some of the groups did not pass that requirement.

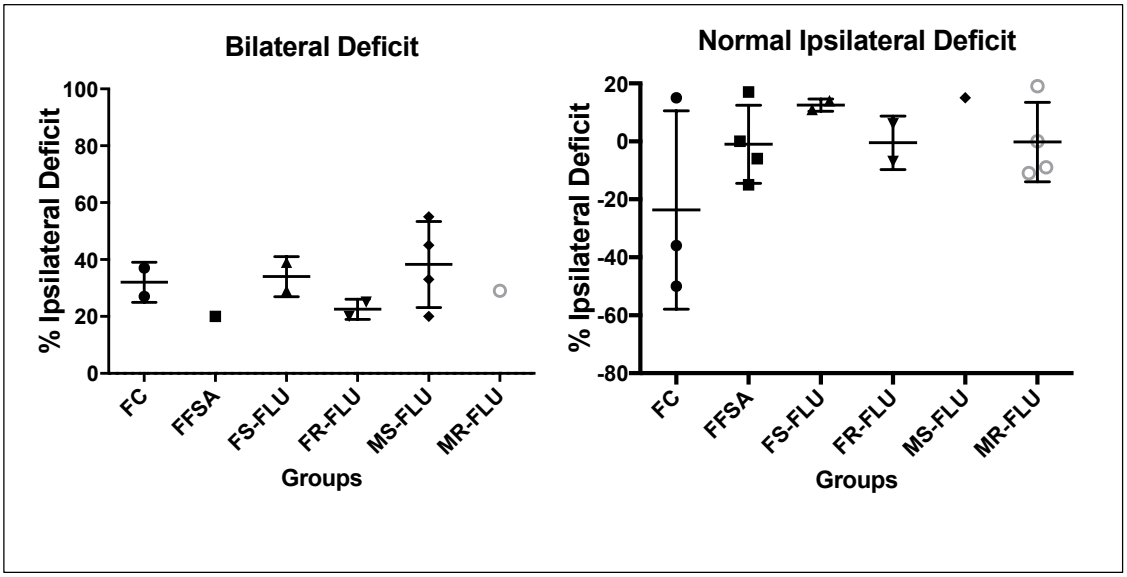

Figure 12 Graphs showing percent bilateral and percent ipsilateral deficit. Graph on the left indicates percent bilateral deficit which includes animals that had more than or equal to 20% contralateral and ipsilateral deficit. The graph on the right shows percent ipsilateral deficit which includes animals that had less than 20% ipsilateral deficit. Each data point on the graph is representing an individual animal and it is plotted with a wide horizontal bar which represents a group mean with standard deviation error bars. (FC - Female Control, FFSA - Female Fluoxetine, Simvastatin, Ascorbic Acid, FS-flu – Female S-Fluoxetine, FR-flu – Female R-Fluoxetine, MS-flu – Male S-Fluoxetine, MR-flu – Male R-Fluoxetine)

Bilateral deficit is a normalized value obtained by subtracting ipsilateral function value from 1. Graphed on the left in figure 12, only the animals reaching 20% deficit on both sides are included in this part to determine the bilateral deficit of the right paw. The

right graph indicates normal ipsilateral deficit which includes animals with less than 20% ipsilateral deficit. The % ipsilateral deficit values are plotted as a group mean with standard deviation error bars. The negative values associated with the FC (female control) group in the normal ipsilateral deficit graph, indicates that the animals performed better post-stroke with their right paw than they did in pre-stroke training: this only occurs if the animal did not reach a plateau in the Montoya Training. One-way ANOVA analysis could not be performed because it requires each group to have at least two or more data points, and some of the groups did not pass that requirement.

Evans Blue Spectrophotometer Analysis

One milliliter of Evans Blue dye injected during cardio-perfusion of animals is viewed using a spectrophotometer instrument and micro-titer plates containing 120 microliter samples with three replicates. Tissue section containing Evans Blue dye in the cerebral cortex and cerebellum was dissected from each brain sample of each group. Fluorescence was read from each sample with excitation at 620 nm and emission at 680 nm. Fluorescence data was used to calculate microgram/gram of Evans Blue dye in each sample and is plotted on the y-axis in the graphs to follow. The tissue Evans Blue data is calibrated against its corresponding control curve using known amounts of Evans Blue dye. The calibration curve is a control curve bereft of any tissue and was prepared with 1:4 calibrated trichloroacetic acid (TCA) background solution (100 microliters of artificial cerebrospinal fluid (ACSF) in 400 microliters of 50% TCA). Then, 30 microliters of Evans blue dye plus the background stock solution was mixed with 90 microliters of 95% ethanol. Similarly, tissue samples were homogenized in the background stock solution prepared with 1:4 calibrated TCA solution (100 microliters

ACSF in 400 microliters of 50% TCA). Then, 30 microliters of Evans Blue captured in the supernatant was added into 90 microliters of 95% ethanol.

BLANK	**2 μg CALIBRATION**	**5 μg CALIBRATION**	**10 μg CALIBRATION**
1.0 ml BS	998 µl BS	995 µl BS	990 µl BS
0 µl EBBS	2 µl EBBS	5 µl EBBS	10 µl EBBS

Table 5 Preparation of Evans Blue calibrated stock solution. 1mg/1ml of Evans Blue was mixed in the prepared background solution. Three replicates of each were fixed by adding the Evans Blue plus background stock solution minus the tissue, followed by adding 90 microliters of 95% ethanol into each well. (BS = Background solution, EBBS = Evans Blue plus background solution)

The test samples were calibrated against control samples, which contained only the Evans Blue dye plus the background stock solution, devoid of any tissue. As shown in table 5, the calibration was made in the increments of 0, 2, 5 and 10 micrograms. This was obtained by adding respective amounts in microliters of Evans Blue dye in their corresponding amounts in microliters of background stock solution. Total of 1mg/ml of Evans Blue in background stock solution was prepared to add as three replicates in each 96-well micro-titer spectrophotometer plate.

Fluorescence data from each standard curve is used to perform linear regression analysis which yielded slope and the y-intercept of the line. This is used to calculate microgram per 30 microliters of Evans Blue in the micro-titer plate sample. Then, this is converted into microgram per 500 microliters of Evans Blue in the original solution of the sample. The grams of tissue obtained in TCA solution was used to calculate micrograms/gram of Evans Blue tissue. We then plotted these values to interpret our results.

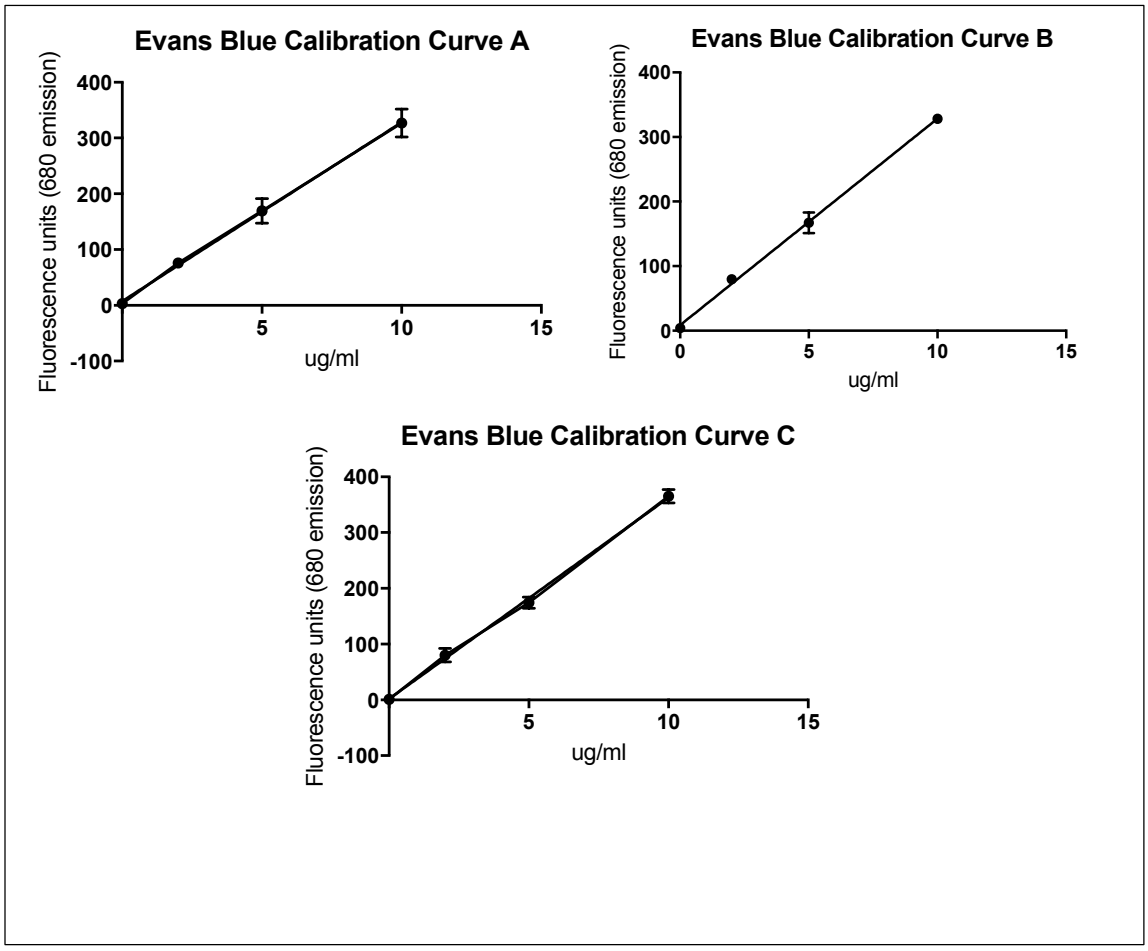

Figure 13 Evans Blue Calibration Curves A, B, C. These are the control curves that contained only the Evans Blue solution prepared in a 1:4 calibrated TCA solution (100µL ACSF + 400µL 50% TCA) and followed by adding 90µL of 95% ethanol The calibrated curves are bereft of any tissue. R2-values for line of good fit for each Curves A, B, and C are 0.9865, 0.9952, and 0.995 respectively.

Figure 13 shows three calibration curves that were obtained against their corresponding test samples in the same micro-titer plate. The calibration curve is a control curve bereft of any tissue and was prepared with 1:4 calibrated TCA solution (100 microliters ACSF in 400 microliters of 50% TCA). Then, 30 microliters of Evans blue dye plus the background stock solution was mixed with 90 microliters of 95% ethanol.

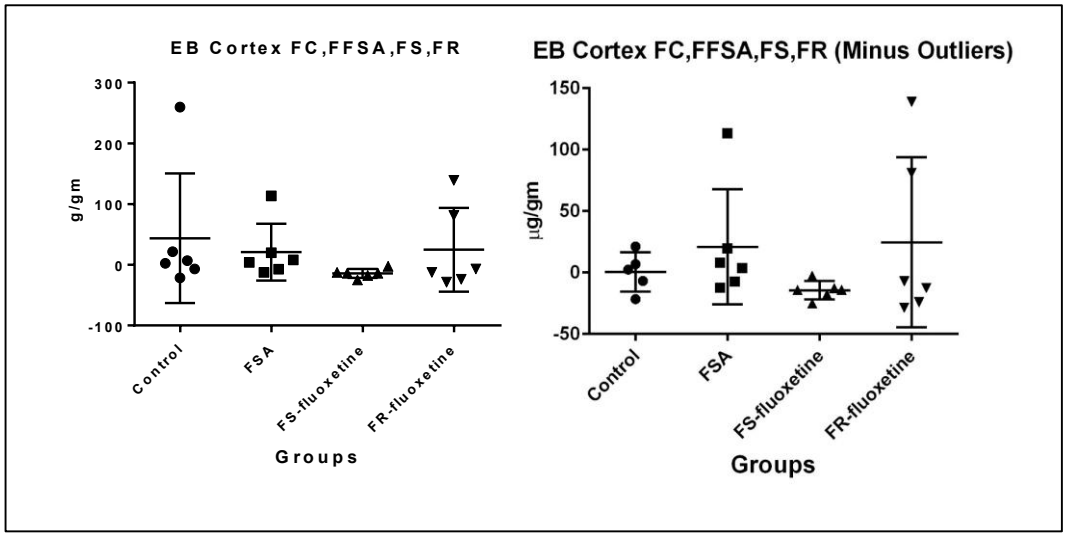

Figure 14 Assessment of BBB permeability by Evans Blue detection in female cerebral cortex. Evans Blue Fluorescence excited at 620nm and emitted at 680nm. This data is calibrated against Curve-A shown in Figure 13. For the left panel of the figure, one-way ANOVA statistical test revealed no significant difference among the group means with *P*-value of 0.5285. The values are plotted with a wide horizontal bar which represents a group mean with standard deviation error bars. The outlier's test identified one outlier in the control group with ROUT analysis of Q=1.000%. The right panel of the graph has no outliers present as tested using ROUT analysis Q=1.000%. The *P*-value is 0.3962, with no statistical significance detected among differences within the mean according to one-way ANOVA statistical analysis. (FC-Female Control, FFSA-Female Fluoxetine, Simvastatin, Ascorbic Acid, FS-Female S-fluoxetine, FR-Female R-fluoxetine)

Evans Blue fluorescence at the blood brain barrier (BBB) in the cerebral cortex of female groups is graphed in figure 14. There is no evident difference among the groups when compared against each other statistically. Statistical variance of the distribution of the sample means appears to be less in the female S-fluoxetine as compared to control and the other two groups. In the left panel of the figure, it is notable that the administration of FSA showed similar variance to the control group, however the control group had one outlier identified according to the ROUT analysis of Q=1.000%. One-way ANOVA statistical test with an outlier revealed no significant difference among the group means with a *P*-value of 0.5285. This data was calibrated against Curve-A in figure 13.

With an outlier removed from the female control group newly graphed on the right in figure 14, the *P*-value changed from 0.5285 to 0.3962. One-way ANOVA without outliers revealed no significant differences among the mean, as shown in figure 14. The ROUT analysis for outliers of Q=1.000% confirmed no outliers present. Hence, all the groups are statistically similar to each other with some statistical variance present in each group. This data was calibrated against Curve-A shown in figure 13.

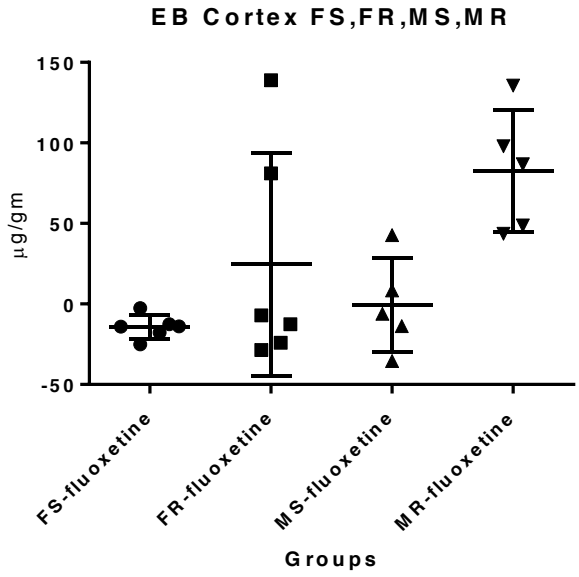

Figure 15 Assessment of BBB permeability by Evans Blue detection in male and female cerebral cortex. Evans Blue Fluorescence excited at 620nm and emitted at 680nm. This data is calibrated against Curve-C shown in Figure 13. The outlier's test identified no outliers present, using ROUT analysis of Q=1.000%. The *P*-value of 0.0091 shows that both male and female S-fluoxetine are statistically significantly different from the male R-fluoxetine with differences within the mean present according to one-way ANOVA statistical analysis. The values are plotted with a wide horizontal bar which represents a group mean with standard deviation error bars. (FS-Female S-fluoxetine, FR-Female R-fluoxetine, MS-Male S-fluoxetine, MR-Male R-fluoxetine)

Interestingly, it can be noted from figure 15 that the Evans blue permeation at the blood brain barrier in the cerebral cortex was less in the female group as well as in the

male group treated with S-fluoxetine compared to male R-fluoxetine group, meaning that the blood brain barrier was not as permeable to Evans Blue dye after stroke induction due to S-fluoxetine in the male and female rats compared to R-fluoxetine in male rats. Unpaired *t*-test with Welch's correction confirms that female S-fluoxetine and male R-fluoxetine are significantly different to each other with a *P*-value of 0.0041. It also confirms that male S-fluoxetine and male R-fluoxetine are significantly different to each other with *P*-value of 0.0045. This graph did not show any outliers present according to the ROUT analysis with Q=1.000%. One-way ANOVA without outliers revealed a significant difference among the means with a *P*-value of 0.0091. Hence, it can be deduced that the R-fluoxetine treatment in male makes the BBB more permeable to Evans Blue. This data is calibrated against Curve-C shown in figure 13.

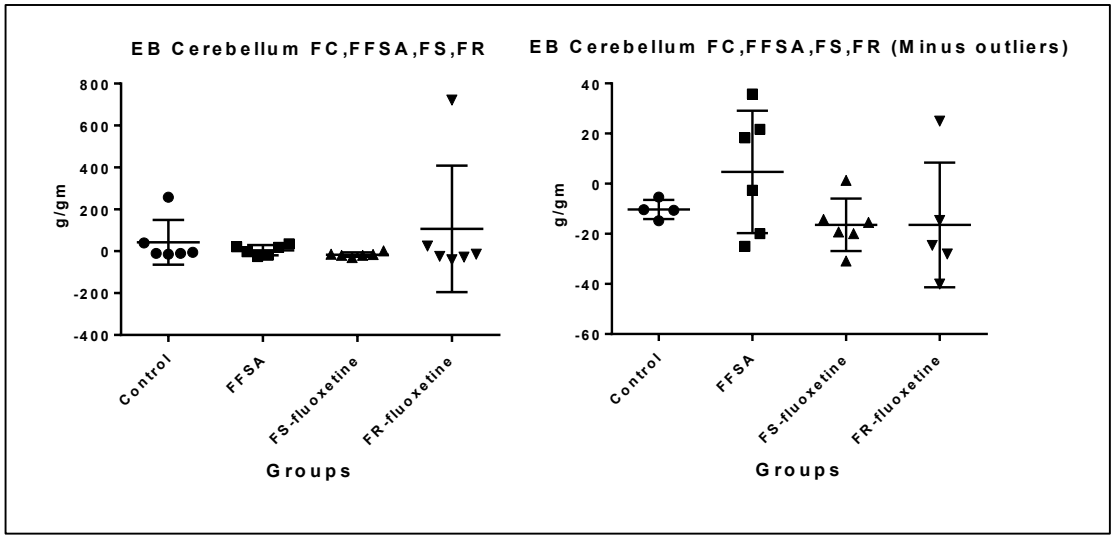

Figure 16 Assessment of BBB permeability by Evans Blue detection in female cerebellum. Evans Blue Fluorescence excited at 620nm and emitted at 680nm. This data is calibrated against Curve-B shown in Figure 13. For the left panel, the outlier's test identified two outliers, one in the control group and one in the females treated with R-fluoxetine group, using ROUT analysis of Q=1.000%. One-way ANOVA revealed no significant differences among the mean with a *P*-value of 0.5772. For the right panel, this graph has no outliers present as tested using ROUT analysis Q=1.000%. The *P*-value is 0.2192, with no statistical significance among differences within the mean according to one-way ANOVA statistical analysis. The values are plotted with a wide horizontal bar which represents a group mean with standard deviation error bars. (FC-Female Control, FFSA-Female Fluoxetine, Simvastatin, Ascorbic Acid, FS-Female S-fluoxetine, FR-Female R-fluoxetine)

As shown in the figure, the control and different female treated groups showed no significant differences in the amount of Evans Blue dye detected in the cerebellum tissue. Figure 16 also indicates that all the groups are statistically similar to each other with some statistical variance present in each group. This data is calibrated against Curve-B graphed in figure 13. For the left panel graph in figure 16, the ROUT analysis showed Q=1.000% with two outliers present, one outlier found in the control group and the other outlier in the R-fluoxetine group. One-way ANOVA with outliers revealed no significant differences among the mean with a *P*-value of 0.5772.

The right panel in figure 16, is a graph re-constructed with two outliers removed. The new Evans Blue fluorescence data graphed shows no statistical difference among

each other. There are no outliers present as assessed using ROUT analysis with Q=1.000%. One-way ANOVA without outliers revealed no significant differences among the mean with a *P*-value of 0.2192. This graph was also calibrated against Curve-B shown in figure 13.

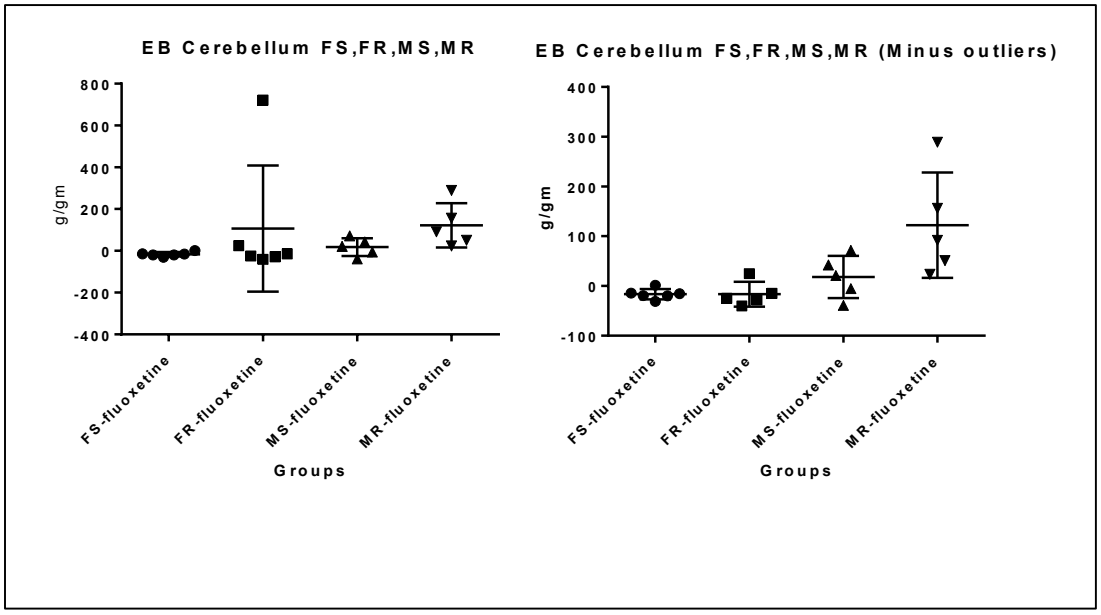

Figure 17 Assessment of BBB permeability by Evans Blue detection in male and female cerebellum. Evans Blue Fluorescence excited at 620nm and emitted at 680nm. This data is calibrated against Curve-C shown in Figure 13. For the left panel, the outlier's test identified one outlier in the female group treated with R-fluoxetine, tested using ROUT analysis of Q=1.000%. The *P*-value is 0.4628, with no detected statistical significance among differences within the mean according to one-way ANOVA statistical analysis. For the right panel, the outlier's test identified no outliers present using ROUT analysis of Q=1.000%. The *P*-value is 0.0031 showing female S- and R-fluoxetine as statistically significantly different from male R-fluoxetine according to one-way ANOVA statistical analysis. The values are plotted with a wide horizontal bar which represents a group mean with standard deviation error bars. (FS-Female S-fluoxetine, FR-Female R-fluoxetine, MS-Male S-fluoxetine, MR-Male R-fluoxetine)

The graph shown in figure 17 indicates the fluorescence of Evans Blue permeation at the blood brain barrier in the cerebellum to study and compare female versus male responses to the fluoxetine enantiomers treatment. Interestingly as seen in

the left panel in figure 17, there is a notable statistical difference present between female S-fluoxetine and male R-fluoxetine, confirmed by an unpaired *t*-test with Welch's correction *P*-value of 0.0423. It shows that the males administered with an R-enantiomer had more Evans Blue fluorescence cross the BBB compared to the S-enantiomer in the females. So, it is possible to conclude that the S-enantiomer of fluoxetine holds the BBB intact after stroke induction in rats. There was one outlier identified using ROUT's analysis with Q=1.000% in this graph. One-way ANOVA with an outlier, revealed no significant difference among the means with *P*-value of 0.4628. This data is calibrated against Curve-C shown in figure 13.

The right panel in figure 17 is a re-constructed graph with the outliers removed. There is a statistical difference present between female S-fluoxetine and male R-fluoxetine, confirmed by an unpaired *t*-test with Welch's correction *P*-value of 0.0423. Also, there is a statistical difference present between female R-fluoxetine and male R-fluoxetine, confirmed by an unpaired *t*-test with Welch's correction *P*-value of 0.0407. Male S-fluoxetine is not statistically different than any other groups graphed in figure 17. This curve did not have any outliers present according to the ROUT analysis with Q=1.000%. One-way ANOVA without any outliers present, revealed a significant difference among the means with a *P*-value of 0.0031. Hence, it can be deduced that females with S- and R-fluoxetine had significantly less Evans Blue permeation at the BBB in the cerebellum compared to male R-fluoxetine, and that the R-fluoxetine in males is less resistant to permeate the dye for crossing BBB after its damage due to stroke induction. This data is calibrated against Curve-C shown in figure 13.

Gene Expression Analysis

Real-time polymerase chain reaction by the method of quantification allows us to study the gene markers activated after stroke induction to assess different factors such as neurogenesis, neuro-inflammation, neuroplasticity, and neuronal cell growth and differentiation. Brain tissue collected and homogenized from the peri-infarct region, was processed into messenger RNA after removing genomic DNA. Then, the mRNA was converted into complementary DNA, which was then transferred into RT-PCR custom-designed well plates for quantitative real-time PCR analysis which revealed the Ct values. A Ct-value is the number of RT-PCR cycles crossing the set threshold value. For example, *Arg1* with a Ct-value of 26.2 indicates that many cycles it took for *Arg1* to reach the set threshold. The gene expression yield is higher when the threshold value is crossed by the signal in less number of cycles at a given time. Threshold value was manually set the same across all groups tested in this part of study to allow comparison of the gene expression. The Ct-values are used for RT-PCR data analysis to yield gene fold-regulation that is interpretable to deduce conclusions. Gene fold-change is obtained in this manner: first, delta Ct-value is calculated between the gene of interest and housekeeping gene for each experiment. Then, the average delta Ct-values between experiments (replicates) is calculated. Next, the delta-delta Ct-values are calculated using the equation: delta Ct experiment – delta Ct control. Then, the fold change is calculated as 2^(-delta delta Ct). Fold-change is the normalized gene expression in the sample group divided by the normalized gene expression in the control group. Fold-change values greater than 1 indicate up-regulation. On the contrary, fold-change values less than 1

indicate down-regulation. The housekeeping genes that were used for normalization of calculations and comparisons were *Hprt1* and *Ldha*.

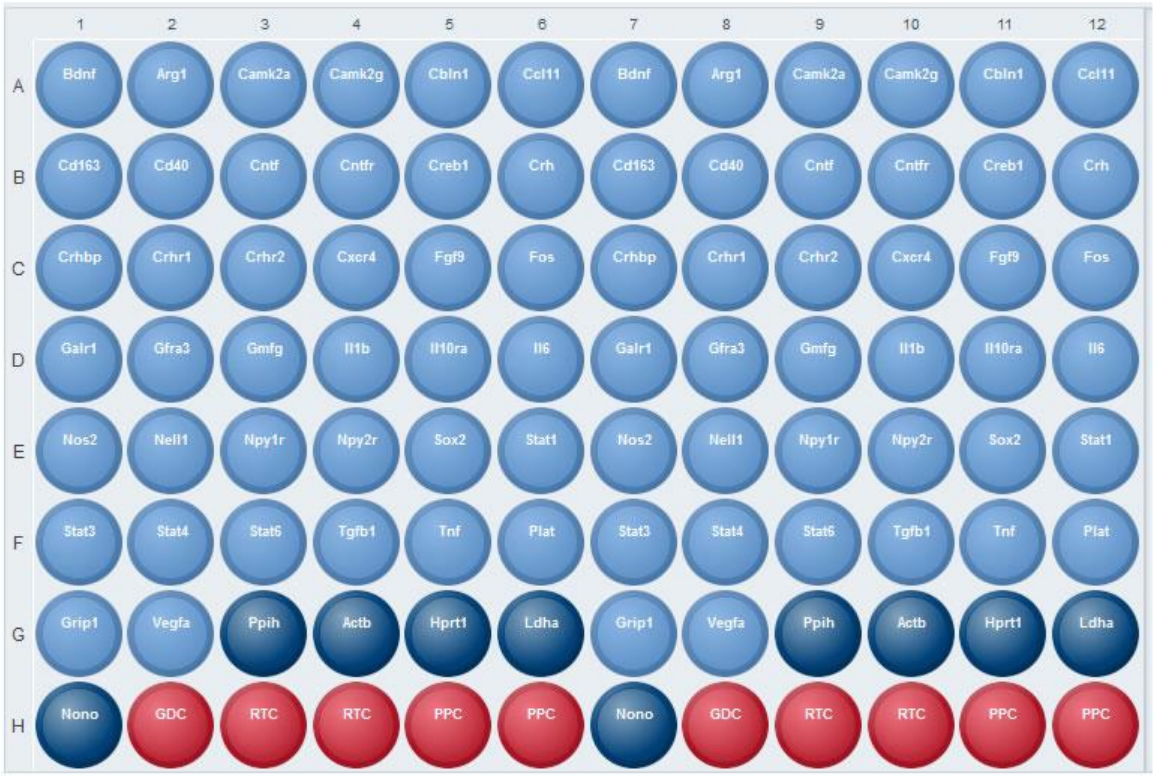

Figure 18 Custom RT-PCR 96-well plate designed to study gene expression. This plate contains primers for genes chosen to study microglial subtypes involved in neuro-inflammation, neurogenesis factors, and neuroplasticity. Each gene has a duplicate. (Light blue wells – genes of interest, dark blue wells – housekeeping genes, red wells – control wells). Control wells include GDC – genomic DNA contamination, RTC – reverse transcription control, and PPC – positive PCR control.

Figure 18 is a picture depicting the custom-made 96-well RT-PCR plate used in this part of study. Each gene has one more replicate (total two) on the plate to ensure accuracy. Treated groups are compared against the control group, as well as against their female or male counterparts. This allows us to compare and contrast the gene markers between groups to conclude their contribution in neurogenesis factors.

In this part of study, taking the average of replicates of gene markers pass as statistically significant if one replicate is above the blue line (marking statistical

significance) and the other replicate is slightly below the blue line. If both replicates of genes are strictly up-regulated or down-regulated then those results give more confidence, while one replicate of the gene up-regulated but other one down-regulated or vice-versa gives less confidence.

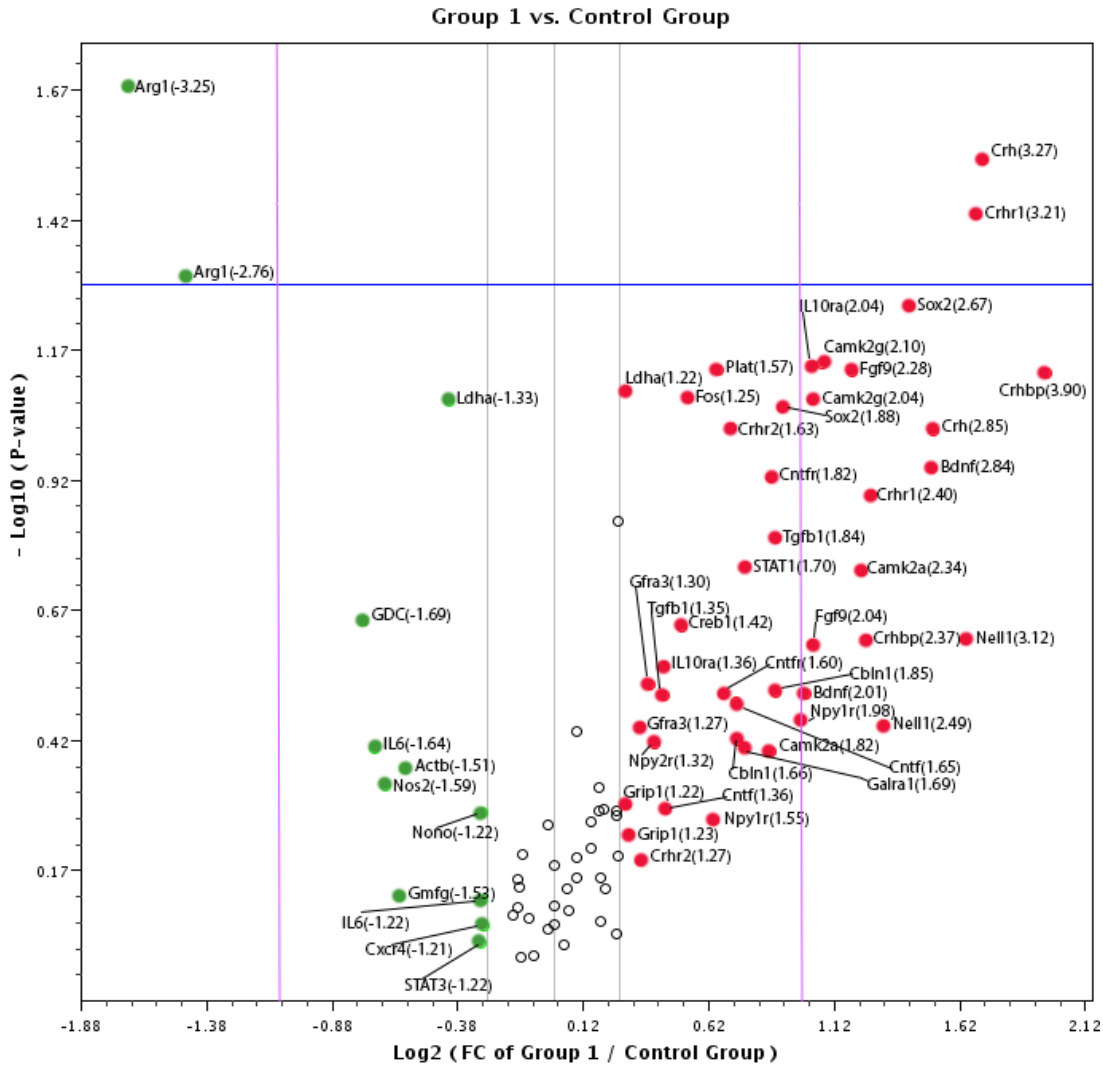

Figure 19 Volcano Plot comparing RT-PCR gene markers active after stroke between female control group and female FSA group. Each gene has one more replicate on well plate. The threshold value was kept same across the two groups. Control represents female control group untreated with any medication, and Group1 represents female group treated with FSA (fluoxetine, simvastatin, and ascorbic acid). Red data points indicate up-regulated gene markers, and green data points indicate down-regulated gene markers. Black uncolored data points indicate unchanged gene markers between the two assessed groups. The blue horizontal line demarcates statistical significance: data points above are statistically significant (*P*<0.05) and those below are statistically insignificant (*P*>0.05). Gene

markers on both sides outside of the pink vertical lines are considered significant genes which change more than 2 fold. Numbers in brackets indicate fold-regulation.

Up-regulated	Down-regulated
*Crh**(3.27) *Crhr1**(3.21)	*Arg1*# (-3.25, -2.76)
Camk2g # (2.10, 2.04) *Fgf9* # (2.04, 2.28) *Crhbp* # (2.37, 3.90) *Crh* # (3.27, 2.85) *Nell1* # (3.12, 2.49) *Bdnf* # (2.84, 2.01) *Crhr1* * (2.40) *Il10ra* # (2.04, 1.36) *Camk2a* # (2.34, 1.82) *Sox2* # (1.88, 2.67) *Crhr2* # (1.27, 1.63) *Ldha* * (1.22) *Fos* * (1.45) *Plat* * (1.57) *Tgfb1* # (1.35, 1.85) *Stat1* * (1.70) *Creb1* * (1.42) *Cntfr* # (1.82, 1.60) *Galra1* * (1.69) *Grip1* # (1.23, 1.22) *Cbln1* * (1.66) *Npy1r* # (1.98, 1.55) *Npy2r* * (1.32)	*Ldha* *(-1.33) *Il-6* # (-1.64, -1.22) *Actb* *(1.51) *Nos2* *(-1.59) *Gmfg* *(-1.53) *Cxcr4* *(-1.21) *Stat3* *(-1.22) GDC *(-1.69) *Nono* *(-1.22)

Table 6 Gene markers that are up-regulated and down-regulated in the female control group versus female FSA (fluoxetine, simvastatin, and ascorbic acid) group. At the top of the table, genes with *P*-values less than 0.05 are shown. At the bottom of the table, any gene which changes more than 2 fold is also considered a significant change (highlighted in yellow); rest of the gene markers are not statistically significant. # denotes both replicates of the gene, and * denotes one of the two replicates of the gene. Fold-regulation for each gene marker is indicated in brackets. The blue line demarcates statistical significance: gene markers listed above are statistically significant and those below are statistically insignificant as far as the *P*-value goes only.

As seen in figure 19, the female group treated with FSA (fluoxetine, simvastatin, and ascorbic acid) for 6 days after surgery until sacrificed on 7th day, is compared against the female control group untreated with any of the FDA approved drugs. Both groups comprise of six rats each. The graph indicates that both replicates of Arginase1 were statistically significant and down-regulated (green), while one replicate each of *Crh* and

Crhr1 were also statistically significant and up-regulated (red). The increase of *Crh* and *Crhr1* indicates an increased amount of stress after stroke. A decrease in *Arg1* indicates a decrease in either M2a or M2c microglia, both of which regulate anti-inflammation. Horizontal blue line on the graph divides the above gene markers as statistically significant with *P*-value less than 0.05, and those below are statistically insignificant with *P*-value greater than 0.05. Gene markers plotted on both sides outside of the pink vertical lines are significant with changes more than 2-fold. Several growth factors are significantly up-regulated, but we also see a down-regulation of *Arg1*; this suggests that either the microglial markers chosen in this project do not correspond to the subtypes of macrophages in the periphery, or the increase in *Bdnf* is not due to microglial polarization.

Table 6 lists the names of gene markers that were up-regulated or down-regulated in female FSA group against female control group. Also, # sign in the table denotes both replicates of a gene, while * denotes one of the two replicates of a gene. Fold-regulation for each gene marker is indicated in the brackets. Significant genes highlighted in the table changed more than 2-fold. These genes were up-regulated and include growth factors such as *Sox2*, *Fgf9*, *Bdnf*, *Nell1;* synaptic plasticity markers such as *Camk2a* and *Camk2g,* stress markers such as *Crhbp*, *Crh*, *Crhr1*; and a cytokine marker, *Il10ra*. The results of the up-regulated genes expressed which were non-significant ($P>0.05$) include M1 microglial marker, *Stat1*; and other cytokine markers such as *Tgfb1*, *Fos*, *Camk2a, Creb1*, *Cntfr*, *Grip1*, *Il10ra, Sox2* and *Cbln1*. The up-regulation of *Plat*, *Galra1*, *Npy1r*, *Ldha*, and *Crhr2* was also notable.

Several non-significantly down-regulated gene markers include *Nos2*, *Il-6*, *Stat3*, *Gmfg*, *Cxcr4*, *Nono*, *Actb*, and *Ldha*.

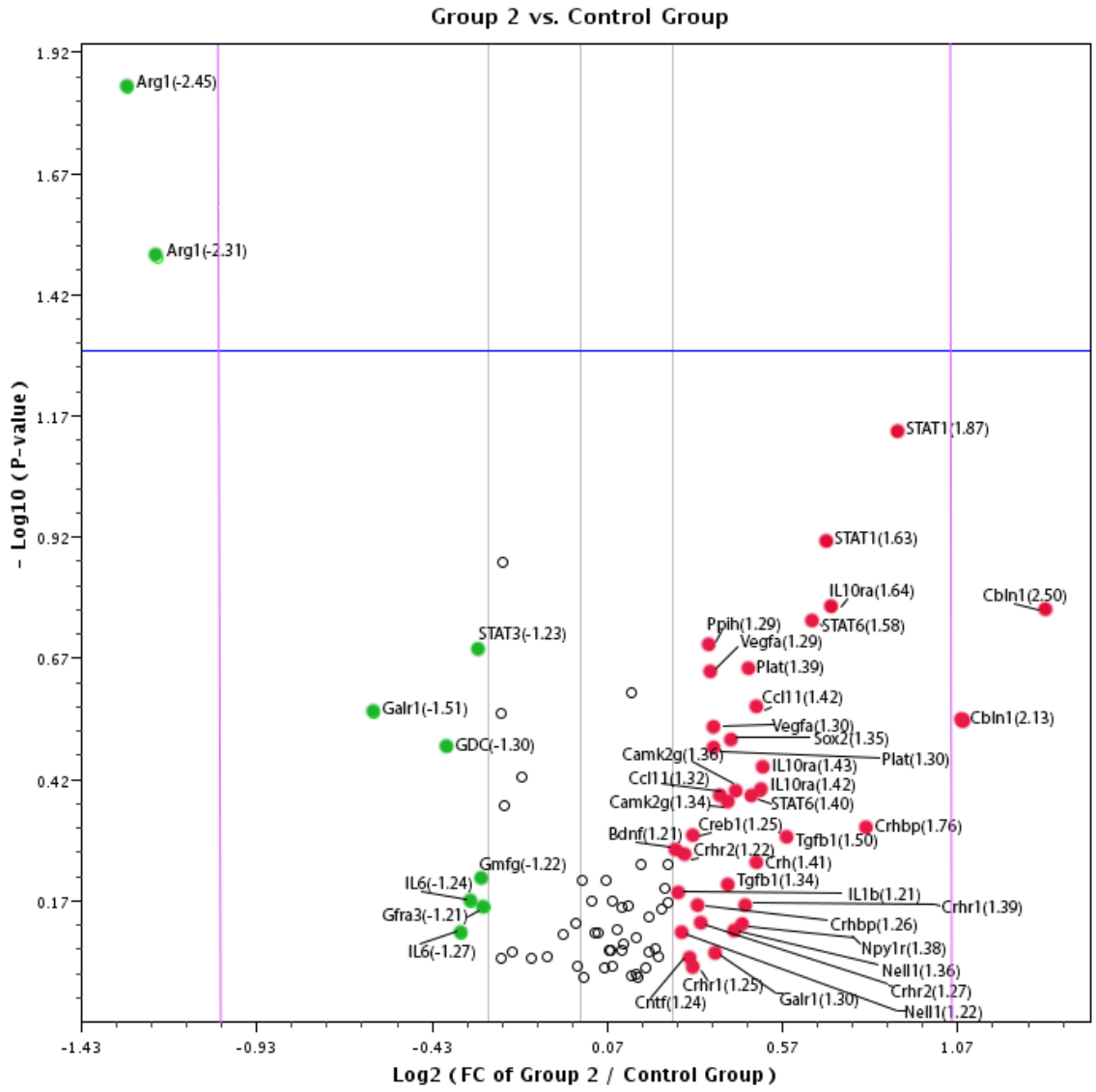

Figure 20 Volcano Plot comparing RT-PCR gene markers active after stroke between female control group and female S-fluoxetine group. Each gene has one more replicate on well plate. The threshold value was kept same across the two groups. Control represents female control group untreated with any medication, and Group2 represents female group treated with S-fluoxetine. Red data points indicate up-regulated gene markers, and green data points indicate down-regulated gene markers. Black uncolored data points indicate unchanged gene markers between the two assessed groups. Numbers in brackets indicate fold-regulation. The blue line demarcates statistical significance: data points above are statistically significant (*P*<0.05) and data points below are statistically insignificant (*P*>0.05). Gene markers on both sides outside of the pink vertical lines are considered significant which change more than 2 fold.

Up-regulated	Down-regulated
	Arg1# (-2.45, -2.31)
Cbln1 # (2.50, 2.13) *Camk2g*# (1.36, 1.34) *Ccl11* # (1.42, 1.32) *Bdnf* * (1.21) *Cntf* * (1.24) *Crh* * (1.41) *Creb1* * (1.25) *Crhbp* # (1.26, 1.76) *Crhr1* # (1.39, 1.25) *Crhr2* # (1.22, 1.27) *Il-1b* # (1.42, 1.21) *I10ra* # (1.43, 1.64) *Galr1* * (1.30) *Nell1* # (1.22, 1.36) *Sox2* * (1.35) *Stat1* * (1.63) *Npy1r* * (1.38) *Stat6* # (1.58, 1.40) *Tgfb1* # (1.34, 1.50) *Plat* # (1.39, 1.30) *Vegfa* # (1.30, 1.29) *Ppih* * (1.29)	*Galr1* * (-1.51) *Gmfg* * (-1.22) *Il-6* # (-1.24, -1.27) *Gfra3* * (-1.21) *Stat3* * (-1.23) GDC # (-1.31, -1.31)

Table 7 Gene markers that are up-regulated and down-regulated in the female control group versus female S-fluoxetine group. At the top of the table, significant gene with *P*-value less than 0.05 is shown. At the bottom of the table, any gene which changes more than 2 fold is also considered a significant change (highlighted in yellow); rest of the gene markers are not statistically significant. # denotes both replicates of the gene, and * denotes one of the two replicates of the gene. Fold-regulation for each gene marker is indicated in brackets. The blue line demarcates statistical significance: gene markers listed above are statistically significant and those below are statistically insignificant as far as *P*-value goes only.

Figure 20 is a volcano plot indicating the gene expression of the female group treated with S-fluoxetine compared against the female control group. The female control group comprises of six rats while the female S-fluoxetine group comprises of 5 rats. The graph indicates that both replicates of *Arg1* is statistically significant and is down-regulated (green), which shows a decrease in M2 anti-inflammatory microglia. So, we can deduce that administration of S-fluoxetine lowered anti-inflammation by decreasing

M2 microglia in the female group. Horizontal blue line on the graph divides the above gene markers as statistically significant with *P*-value less than 0.05, and those below are statistically insignificant with *P*-value greater than 0.05. Gene markers plotted on both sides outside of the pink vertical lines are significant with changes more than 2-fold.

Table 7 is a list of the genes up-regulated and down-regulated for female S-fluoxetine group compared to the female control group. *Cbln1* is a significant gene which changes more than 2-fold. Genes that were non-significant and up-regulated include microglial M1 markers *Ccl11*, *Il-1b*, and *Stat1* in addition to M2 markers *Tgfb1* and *Stat6*. Others that were notable include *Il10ra*, growth factors such as *Bdnf*, *Nell1*, *Sox2*, *Tgfb1*, *Vegfa*, *Camk2g*, *Creb1*, *Cntf*; others such as *Plat*, *Galra1*, *Npy1r*, and *Ppih*; and some stress markers such as *Crhbp*, *Crh*, *Crhr1*, and *Crhr2*.

Non-significant down-regulated gene markers include *Gmfg*, *Gfra3*, and *Galr1*; and some microglial markers including *Il-6*, and *Stat3*.

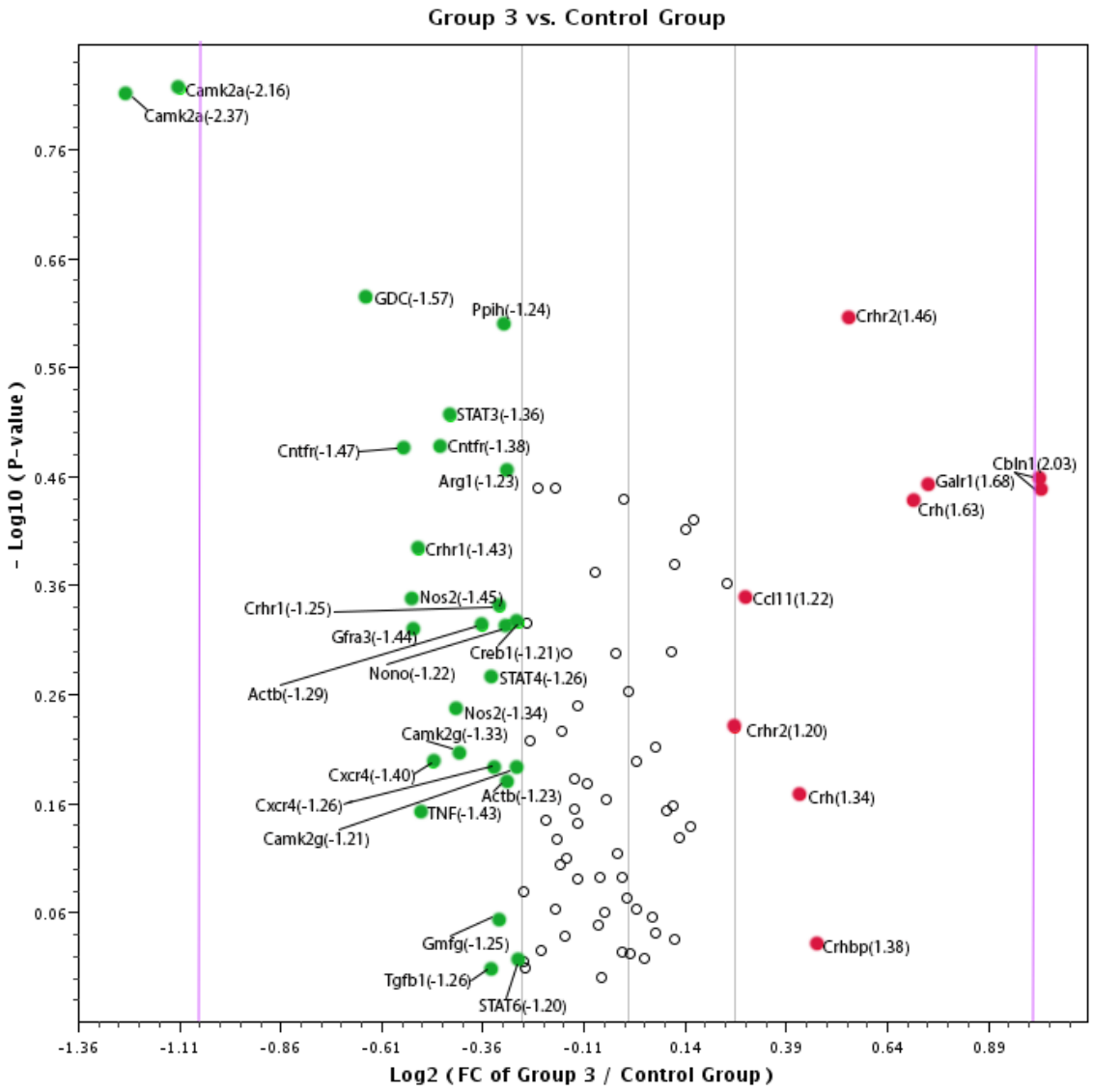

Figure 21 Volcano Plot comparing RT-PCR gene markers active after stroke between female control group and female R-fluoxetine group. Each gene has one more replicate on well plate. The threshold value was kept same across the two groups. Control represents female control group untreated with any medication, and Group3 represents female group treated with R-fluoxetine. Red data points indicate up-regulated gene markers, and green data points indicate down-regulated gene markers. Black uncolored data points indicate unchanged gene markers between the two assessed groups. Numbers in brackets indicate fold-regulation. All of the gene markers assessed between the two groups are statistically not significant ($P > 0.05$), except the gene markers on both sides outside of the pink vertical lines are considered significant which change more than 2 fold.

Up-regulated	Down-regulated
Cbln1 # (2.03, 2.03)	*Camk2a* # (-2.37, -2.16)
Ccl11 * (1.22)	*Arg1* * (-1.23)
Crh # (1.63, 1.34)	*Camk2g* # (-1.21, -1.33)
Crhr2 # (1.20, 1.46)	*Cntfr* # (-1.47, -1.38)
Crhbp * (1.38)	*Creb1* * (-1.21)
Galr1 * (1.68)	*Crhr1* # (-1.43, -1.25)
	Cxcr4 # (-1.40, -1.26)
	Gfra3 * (-1.44)
	Gmfg * (-1.25)
	Nos2 # (-1.45, -1.34)
	Stat3 * (-1.36)
	Stat6 * (-1.20)
	Tgfb1 * (-1.26)
	Stat4 * (-1.26)
	Tnf * (-1.43)
	Ppih * (-1.24)
	Actb # (-1.29, -1.23)
	Nono * (-1.22)
	GDC # (-1.57, -1.57)

Table 8 Gene markers that are up-regulated and down-regulated in the female control group versus female R-fluoxetine group. These gene markers are not statistically significant (*P*>0.05). Any gene which changes more than 2 fold is considered a significant change (highlighted in yellow). # denotes both replicates of the gene, and * denotes one of the two replicates of the gene. Fold-regulation for each gene marker is indicated in brackets.

Figure 21 depicts a volcano plot of gene markers and their fold-regulation of female R-fluoxetine against female control group. Both groups comprise of six rats each. Table 8 lists the names of gene markers that were up-regulated or down-regulated. All of the gene markers expressed were statistically non-significant with $P>0.05$, except the highlighted genes are significant which change more than 2-fold.

Significant genes were *Cbln1* which is up-regulated, and *Camk2a* which is down-regulated. The results of non-significant up-regulated genes expressed included *Ccl11*, *Crhbp*, *Crh*, *Crhr2*, and *Galr1*. And non-significant down-regulated genes include M2 microglial markers such as *Arg1*, *Stat3*, *Stat6*, *Tgfb1*, and M1 markers such as *Tnf*, *Nos2*, and *Stat4*. *Camk2g* along with *Creb1* and *Cxcr4* are also low. Other notable genes include *Cntfr*, *Tgfb1*, *Crhr1*, *Gfra3*, *Gmfg*, *Nono*, *Actb*, and *Ppih*.

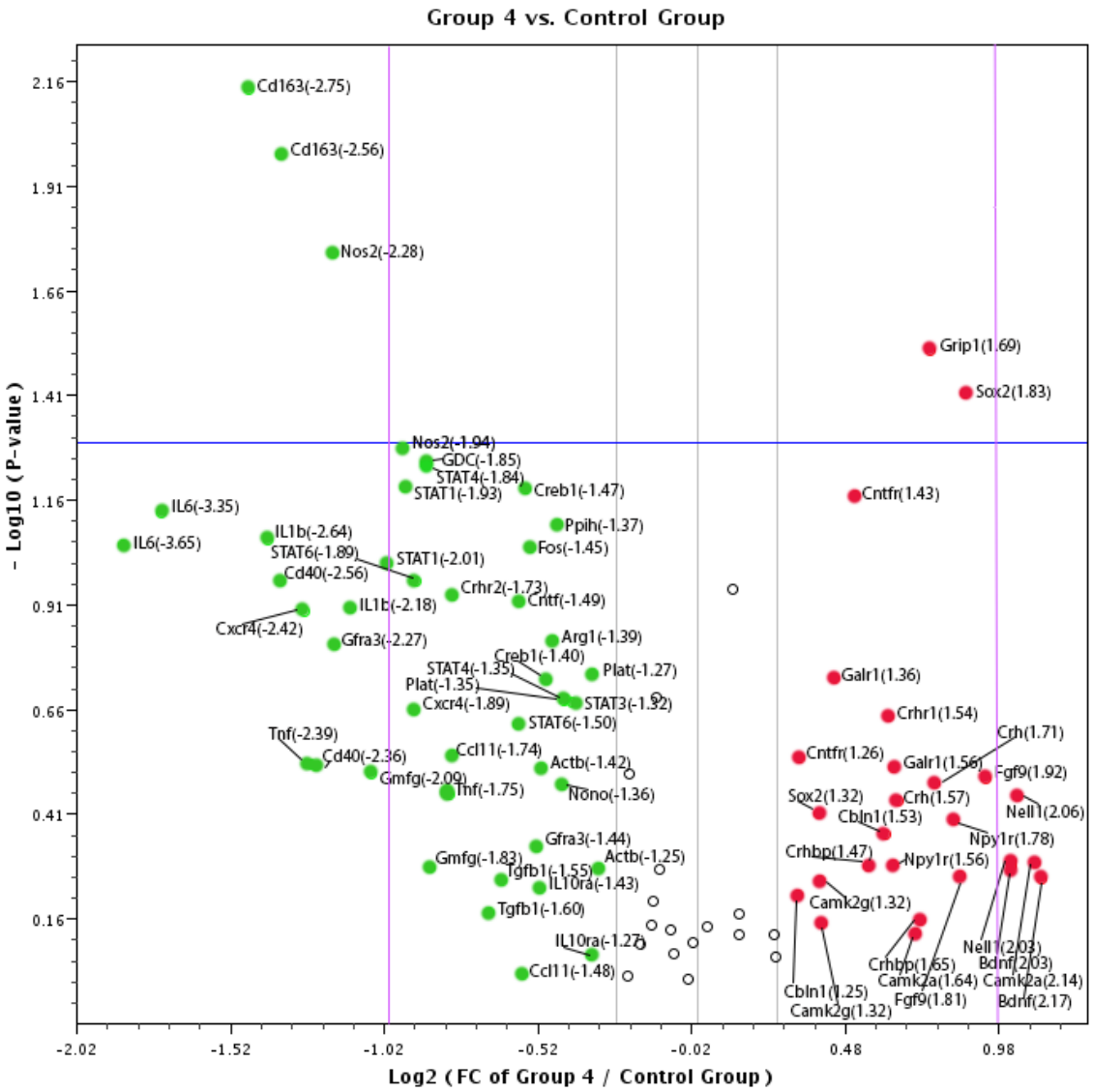

Figure 22 Volcano Plot comparing RT-PCR gene markers active after stroke between female S-fluoxetine group and male S-fluoxetine group. Each gene has one more replicate on well plate. The threshold value was kept same across the two groups. Control represents female S-fluoxetine group and Group4 represents male group treated with S-fluoxetine. Red data points indicate up-regulated gene markers, and green data points indicate down-regulated gene markers. Black uncolored data points indicate unchanged gene markers between the two assessed groups. Numbers in brackets indicate fold-regulation. The blue line demarcates statistical significance: data points above are statistically significant (*P*<0.05) and data points below are statistically insignificant (*P*>0.05). Gene markers on both sides outside of the pink vertical lines are considered significant which change more than 2 fold.

Up-regulated	Down-regulated
*Grip1** (1.69) *Sox2** (1.83)	*Cd163#* (-2.75, -2.56) *Nos2#* (-2.28, -1.94)
Bdnf # (2.03, 2.17) *Nell1 #* (2.06, 2.03) *Camk2a#* (2.14, 1.64) *Camk2g#* (1.32, 1.32) *Cbln1 #* (1.53, 1.25) *Cntfr #* (1.26, 1.43) *Crh #* (1.71, 1.57) *Crhbp #* (1.65, 1.47) *Fgf9 #* (1.81, 1.92) *Crhr1 **(1.54) *Galr1 #* (1.56, 1.36) *Npy1r #* (1.78, 1.56) *Sox2 **(1.32)	*Cd40 #* (-2.56, -2.36) *Il-1b #* (-2.18, -2.64) *Il-6 #* (-3.35, -3.65) *Cxcr4 #* (-2.42, -1.89) *Gfra3 #* (-2.27, -1.44) *Gmfg #* (-2.09, -1.83) *Tnf #* (-2.39, -1.75) *Stat1 #* (-1.93, -2.01) *Arg1 **(-1.39) *Ccl11 #* (-1.74, -1.48) *Cntf **(-1.49) *Creb1 #* (-1.47, -1.40) *Crhr2 **(-1.73) *Fos **(-1.45) *Il-10ra #* (-1.43, -1.27) *Stat3 **(-1.32) *Stat4 #* (-1.84, -1.35) *Stat6 #* (-1.89, -1.50) *Tgfb1 #* (-1.60, -1.55) *Plat #* (-1.27, -1.35) *Ppih **(-1.37) *Actb #* (-1.42, -1.25) *Nono **(-1.36) GDC # (-1.85, -1.85)

Table 9 Gene markers that are up-regulated and down-regulated in the female S-fluoxetine group versus male S-fluoxetine group. At the top of the table, genes with *P*-values less than 0.05 are shown. At the bottom of the table, any gene which changes more than 2 fold is also considered a significant change (highlighted in yellow); rest of the gene markers are not statistically significant. # denotes both replicates of the gene, and * denotes one of the two replicates of the gene. The blue line demarcates statistical significance: gene markers listed above are statistically significant and those listed below are statistically insignificant as far as *P*-value goes only. Fold-regulation for each gene marker is indicated in brackets.

As seen in figure 22, the male group treated with S-fluoxetine is compared against the female S-fluoxetine group. Both groups comprise of five rats each. The graph indicates two replicates of both *Cd163* and *Nos2* are statistically significant and down-regulated (green), while *Grip1* and *Sox2* are also statistically significant and up-regulated (red). *Cd163* shows decreased anti-inflammatory microglia, and on the other hand, *Nos2* shows decreased pro-inflammatory microglia. In this case, it cannot be deduced with

certainty that which one of the two microglial subtypes was dominating due to S-fluoxetine treatment in male group compared to female group. *Grip1* is a factor involved in cell signaling, while *Sox2* is implicated in stem cell maintenance, both of which are increased. Horizontal blue line on the graph divides the above gene markers as statistically significant with *P*-value less than 0.05, and those below are statistically insignificant with *P*-value greater than 0.05. Gene markers plotted on both sides outside of the pink vertical lines are significant with changes more than 2-fold.

Table 9 is a list of the gene markers that were up-regulated and down-regulated when compared the female S-fluoxetine versus male S-fluoxetine groups. Significant genes that were up-regulated include growth factors *Bdnf* and *Nell1*, and cam-kinase *Camk2a*. Non-significant up-regulated markers included growth factors such as *Fgf9* and *Sox2*. *Camk2a* and *Camk2g* in addition to *Cntfr*, *Cbln1*, *Npy1r* and stress markers such as *Crh*, *Crhr1* and *Crhbp* were also notable.

Significant genes that were down-regulated include *Cd40*, *Cxcr4*, *Gmfg*, *Gfra3*, *Il-1b*, *Il-6*, *Stat1*, and *Tnf*. Several genes were non-significant and down-regulated between female S-fluoxetine and male S-fluoxetine groups. Most of those gene markers are implicated in inflammation including *Stat1*, *Stat4*, *Arg1*, *Stat3*, and *Stat6*. Others included are *Il-10ra*, *Ccl11*, *Cntf*, *Cxcr4*, *Fos*, *Gmfg*, *Gfra3*, *Tnf,* and *Tgfb1*. Additionally, *Creb1*, *Crhr2*, *Plat*, *Nono*, *Actb*, and *Ppih* were also notable.

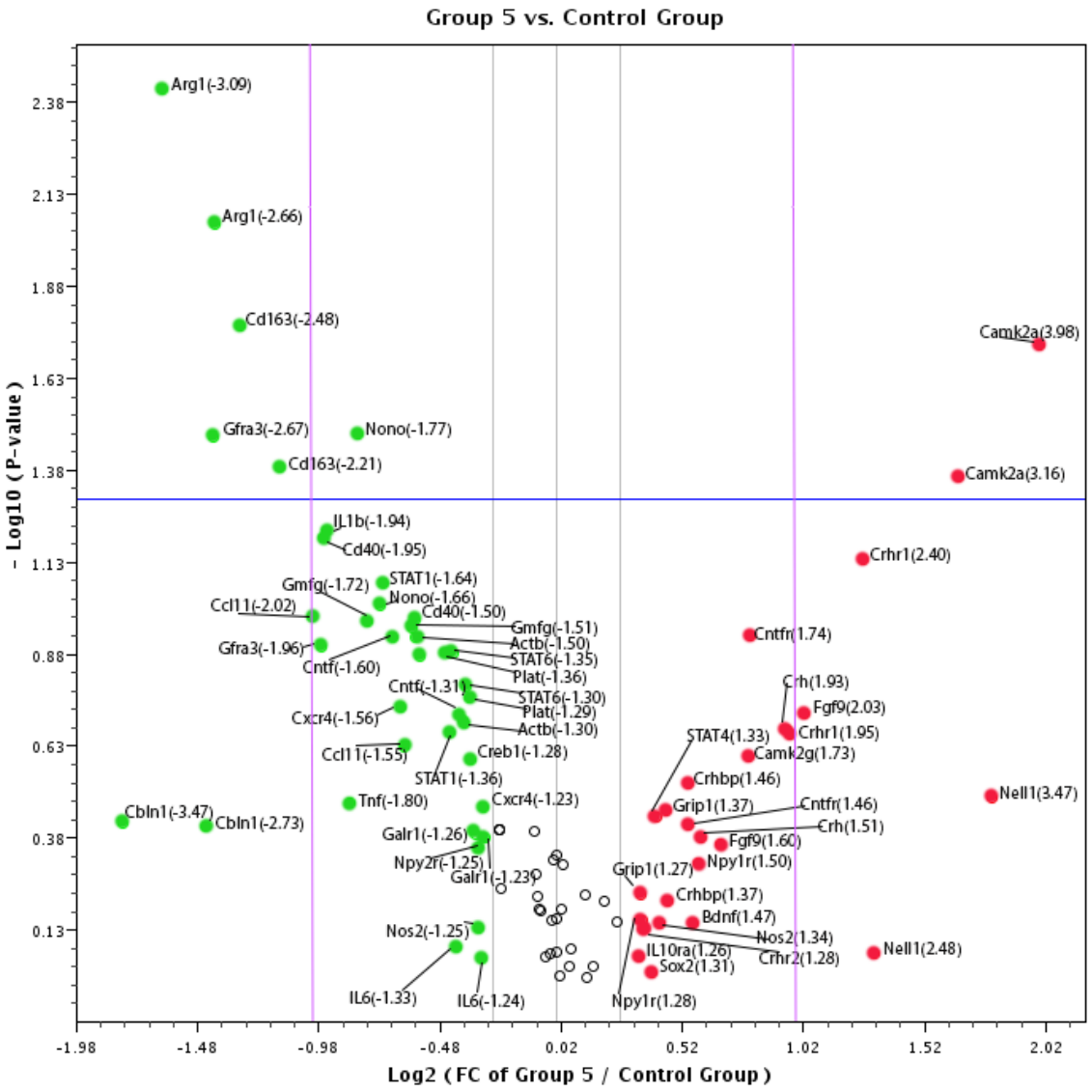

Figure 23 Volcano Plot comparing RT-PCR gene markers active after stroke between female R-fluoxetine group and male R-fluoxetine group. Each gene has one more replicate on well plate. The threshold value was kept same across the two groups. Control represents female R-fluoxetine group, and Group5 represents male group treated with R-fluoxetine. Red data points indicate up-regulated gene markers, and green data points indicate down-regulated gene markers. Black uncolored data points indicate unchanged gene markers between the two assessed groups. Numbers in brackets indicate fold-regulation. The blue line demarcates statistical significance: data points above are statistically significant (*P*<0.05) and data points below are statistically insignificant (*P*>0.05). Gene markers on both sides outside of the pink vertical lines are considered significant which change more than 2 fold.

Up-regulated	Down-regulated
Camk2a# (3.16, 3.98)	*Arg1#* (-3.09, -2.66) *Cd163#* (-2.48, -2.21) *Nono** (-1.77) *Gfra3** (-2.67)
Nell1 # (2.48, 3.47) *Crhr1* # (1.95, 2.40) *Fgf9* # (1.60, 2.03) *Bdnf* * (1.47) *Camk2g** (1.73) *Cntfr* # (1.46, 1.74) *Crh* # (1.51, 1.93) *Crhbp* # (1.37, 1.46) *Crhr2* * (1.28) *Il-10ra* * (1.26) *Npy1r* # (1.28, 1.50) *Nos2* * (1.34) *Sox2* * (1.31) *Stat4* * (1.33) *Grip1* # (1.27,1.37)	*Cbln1* # (-2.73, -3.47) *Ccl11* # (-1.55, -2.02) *Cd40* # (-1.95, -1.50) *Cntf* # (-1.60, -1.31) *Creb1* * (-1.28) *Cxcr4* # (-1.56, -1.23) *Galr1* # (-1.26, -1.23) *Gfra3* * (-1.96) *Gmfg* # (-1.72, -1.51) *Il-1b* # (-1.94, -1.48) *Il-6* # (-1.33, -1.24) *Nos2* * (-1.25) *Stat1* # (-1.36, -1.64) *Npy2r* * (-1.25) *Stat6* # (-1.35, -1.30) *Tnf* * (-1.80) *Plat* # (-1.36, -1.29) *Actb* # (-1.50, -1.30) *Nono* * (-1.65)

Table 10 Gene markers that are up-regulated and down-regulated in the female R-fluoxetine group versus male R-fluoxetine group. At the top of the table, genes with *P*-values less than 0.05 are shown. At the bottom of the table, any gene which changes more than 2 fold is also considered a significant change (highlighted in yellow); rest of the gene markers are not statistically significant. # denotes both replicates of the gene, and * denotes one of the two replicates of the gene. The blue line demarcates statistical significance: gene markers listed above are statistically significant and those listed below are statistically insignificant as far as *P*-value goes only. Fold-regulation for each gene marker is indicated in brackets.

As seen in figure 23, the female group treated with R-fluoxetine is compared against the male group treated with R-fluoxetine. The female R-fluoxetine group comprises of six rats while the male R-fluoxetine comprise of five rats. The graph indicates two replicates of *Arg1* and *Cd163*, and one replicate of *Gfra3* and *Nono* are statistically significant and down-regulated (green), while two replicates of *Camk2a* is also statistically significant and is up-regulated (red). Both *Arg1#* and *Cd163#* show a decrease in M2 anti-inflammatory microglia in male R-fluoxetine compared to their female counterpart. Hence, it can be deduced with certainty that the R-fluoxetine in male

group lowered anti-inflammatory microglia compared to that in female group. *Gfra3* affects to decrease glial cell-derived neuro-trophic factor. *Nono* is implicated in gene transcription. The up-regulation of *Camk2a* shows increased cellular signaling due to increase in calcium release. Horizontal blue line on the graph divides the above gene markers as statistically significant with *P*-value less than 0.05, and those below are statistically insignificant with *P*-value greater than 0.05. Gene markers plotted on both sides outside of the pink vertical lines are significant with changes more than 2-fold.

Table 10 lists the names of gene markers which were up-regulated and down-regulated in the comparison of male R-fluoxetine group against female R-fluoxetine control group. Significant up-regulated genes include growth factors such as *Nell1* and *Fgf9*, and a stress marker *Crhr1*. Non-significant up-regulated genes have several growth factors involved. Up-regulated gene markers include *Bdnf*, *Cntfr*, *Fgf9*, *Sox2*, *Crh*, *Crhr1*, *Crhbp*, and *Crhr2*. Others also notable are *Stat4*, *Nos2*, *Il-10ra*, *Npy1r*, *Camk2g*, and *Grip1*.

Significant down-regulated markers include two genes: *Cbln1*, and *Ccl11*. Non-significant down-regulated genes include microglial markers such as *Il-1b*, *Il-6*, *Ccl11*, *Nos2*, *Stat1*, *Stat6*, and *Tnf*. Also notable were *Cd40*, *Cntf*, *Npy2r*, *Actb*, *Creb1*, *Cxcr4*, *Galr1*, *Gfra3*, *Gmfg*, *Plat*, and *Nono*.

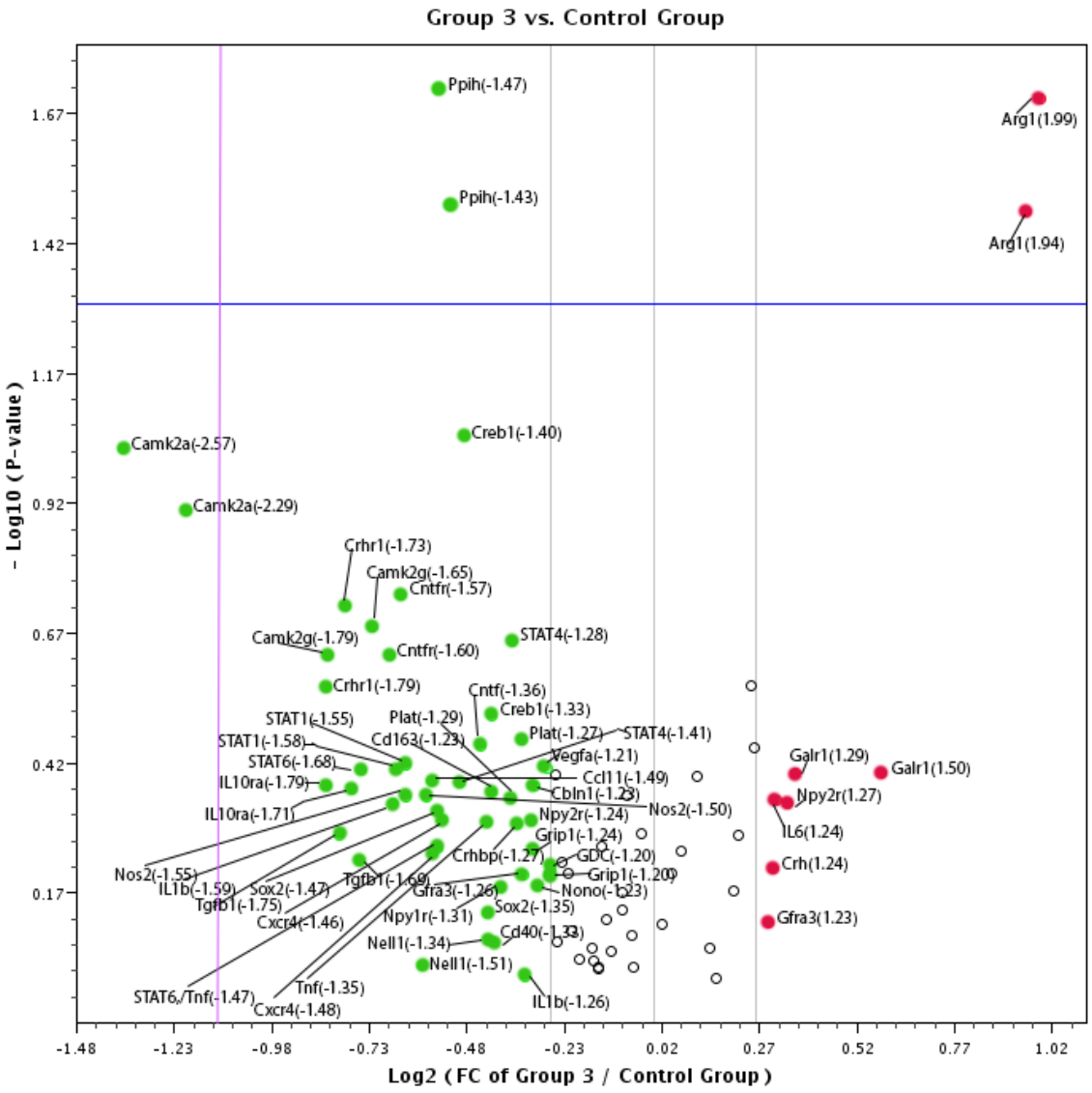

Figure 24 Volcano Plot comparing RT-PCR gene markers active after stroke between female S-fluoxetine group and female R-fluoxetine group. Each gene has one more replicate on well plate. The threshold value was kept same across the two groups. Control represents female S-fluoxetine group, and Group3 represents female group treated with R-fluoxetine. Red data points indicate up-regulated gene markers, and green data points indicate down-regulated gene markers. Black uncolored data points indicate unchanged gene markers between the two assessed groups. Numbers in brackets indicate fold-regulation. The blue line demarcates statistical significance: data points above are statistically significant (*P*<0.05) and data points below are statistically insignificant (*P*>0.05). Gene markers on the left of the pink vertical line are considered significant which change more than 2-fold.

Up-regulated	Down-regulated
Arg1# (1.99, 1.94)	*Ppih*# (-1.47, -1.43)
Crh * (1.24)	*Camk2a*# (-2.57, -2.29)
Galr1 # (1.50, 1.29)	*Camk2g*# (-1.65, -1.79)
Gfra3 * (1.23)	*Cbln1* * (-1.23)
Il-6 * (1.24)	*Ccl11* * (-1.49)
Npy2r * (1.27)	*Cd163* * (-1.33)
	Cd40 * (-1.33)
	Cntf * (-1.36)
	Cntfr # (-1.60, -1.57)
	Creb1 # (-1.33, -1.40)
	Crhr1 # (-1.79, -1.73)
	Cxcr4 # (-1.48, -1.46)
	Gfra3 * (-1.26)
	Il-1b # (-1.26, -1.59)
	Il-10ra # (-1.71, -1.79)
	Nos2 # (-1.55, -1.50)
	Nell1 # (-1.34, -1.51)
	Npy2r * (-1.24)
	Sox2 # (-1.47, -1.35)
	Stat1 # (-1.55, -1.58)
	Npy1r * (-1.31)
	Stat4 # (-1.28, -1.41)
	Stat6 # (-1.47, -1.68)
	Tgfb1 # (-1.69, -1.75)
	Tnf # (-1.35, -1.47)
	Plat # (-1.27, -1.29)
	Grip1 # (-1.20, -1.24)
	Vegfa * (-1.21)
	Nono * (-1.23)
	GDC # (-1.20. -1.20)

Table 11 Gene markers that are up-regulated and down-regulated in the female S-fluoxetine group versus female R-fluoxetine group. At the top of the table, genes with *P*-values less than 0.05 are shown. At the bottom of the table, any gene which changes more than 2 fold is also considered a significant change (highlighted in yellow); rest of the gene markers are not statistically significant. # denotes both replicates of the gene, and * denotes one of the two replicates of the gene. The blue line demarcates statistical significance: gene markers listed above are statistically significant and those listed below are statistically insignificant as far as the *P*-value goes only. Fold-regulation for each gene marker is indicated in brackets.

As seen in figure 24, the female group treated with S-fluoxetine is compared against the female R-fluoxetine group. The female S-fluoxetine group comprise of five rats, while the female R-fluoxetine group comprises of six rats. The graph indicates both

replicates of *Ppih* as statistically significant and down-regulated (green), while both replicates of *Arg1* is also statistically significant and is up-regulated (red). Decreased *Ppih* indicates lowered pre-mRNA splicing during transcription, while increased *Arg1* suggests an increase in M2 anti-inflammatory microglia. Hereby, we can interpret that R-fluoxetine treatment increased anti-inflammation due to up-regulation of M2 microglia in the female group. Horizontal blue line on the graph divides the above gene markers as statistically significant with *P*-value less than 0.05, and those below are statistically insignificant with *P*-value greater than 0.05. Gene markers plotted on left side of the pink vertical line are significant with changes more than 2-fold.

Table 11 lists the names of gene markers which are up-regulated and down-regulated in the comparison of female S-fluoxetine against female R-fluoxetine. Non-significant up-regulated gene markers include *Crh*, *Il-6*, *Galr1*, *Gfra3*, and *Npy2r*.

Camk2a is significant with a change of more than 2-fold and is down-regulated. Others are non-significant. Such down-regulated gene markers include microglial markers such as *Il-1b*, *Nos2*, *Tnf*, *Ccl11*, *Stat1*, *Stat4*, *Cd163*, *Tgfb1* and *Stat6*. Others include *Il-10ra*, *Cd40*, *Camk2g*, *Creb1*, and *Cxcr4*. Additionally, notable genes are *Grip1*, *Cntf*, *Cntfr*, *Vegfa*, *Nell1*, *Gfra3*, *Cbln1*, *Npy1r* and *Npy2r*, *Crhr1*, *Sox2*, *Tgfb1*, *Plat*, and *Nono*.

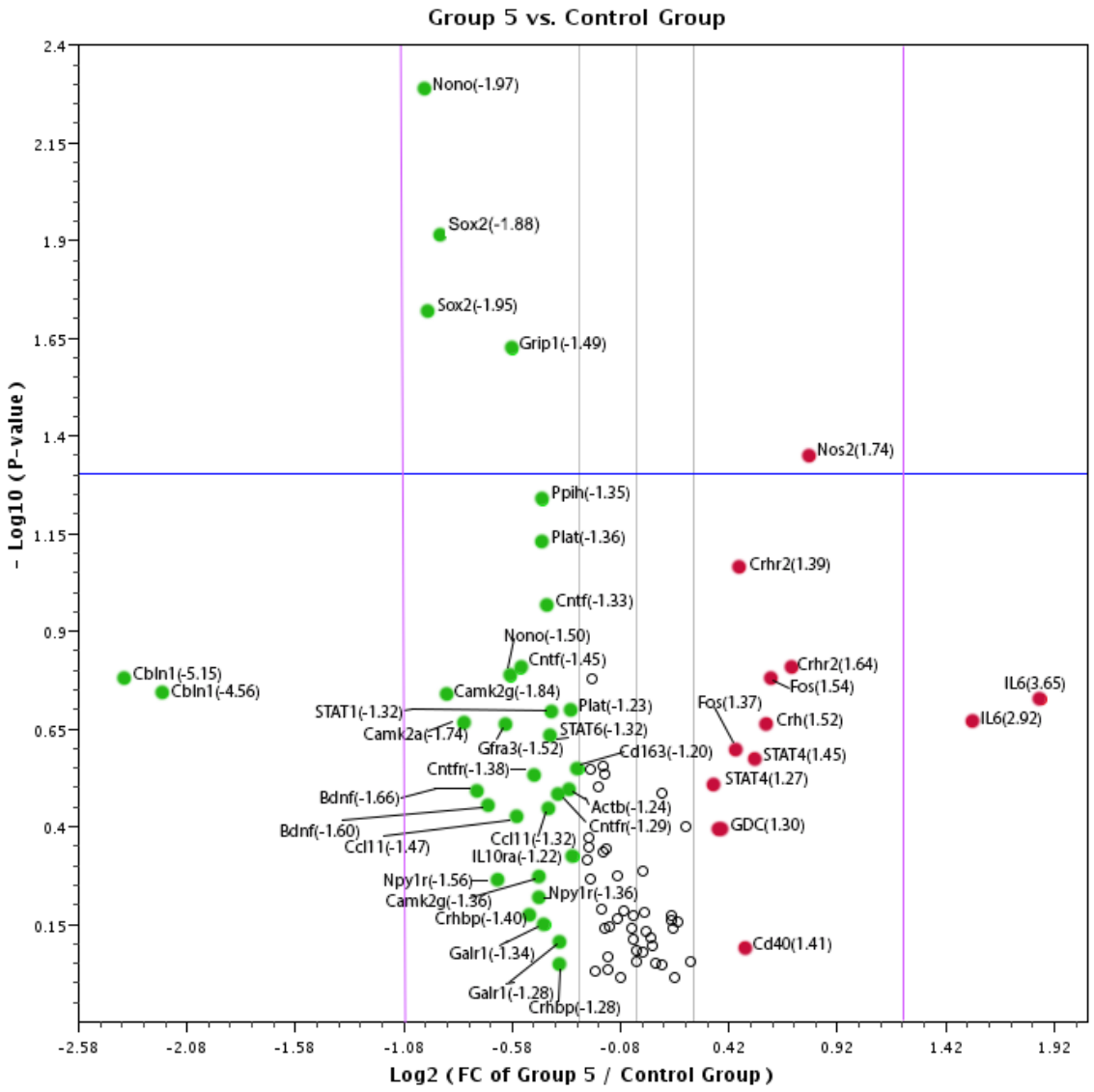

Figure 25 Volcano Plot comparing RT-PCR gene markers active after stroke between male S-fluoxetine group and male R-fluoxetine group. Each gene has one more replicate on well plate. The threshold value was kept same across the two groups. Control represents male S-fluoxetine group, and Group5 represents male group treated with R-fluoxetine. Red data points indicate up-regulated gene markers, and green data points indicate down-regulated gene markers. Black uncolored data points indicate unchanged gene markers between the two assessed groups. Numbers in brackets indicate fold-regulation. The blue line demarcates statistical significance: data points above are statistically significant and data points below are statistically insignificant as far as the *P*-value goes only. Gene markers on both sides outside of the pink vertical lines are considered significant which change more than 2 fold.

Up-regulated	Down-regulated
*Nos2** (1.74)	*Sox2#* (-1.88, -1.95) *Nono** (-1.97) *Grip1** (-1.49)
Il-6 # (2.92, 3.65) *Cd40* * (1.41) *Crh* * (1.52) *Crhr2* # (1.64, 1.39) *Fos* # (1.37, 1.54) *Stat4* # (1.45, 1.27) GDC # (1.30, 1.30)	*Cbln1 #* (-5.15, -4.56) *Bdnf* # (-1.66, -1.60) *Camk2a** (-1.74) *Camk2g#* (-1.84, -1.36) *Ccl11* # (-1.32, -1.47) *Cd163* * (-1.20) *Cntf* # (-1.45, -1.33) *Cntfr* # (-1.38, -1.29) *Crhbp* # (-1.40, -1.28) *Galr1* # (-1.28, -1.34) *Il-10ra* * (-1.22) *Gfra3* * (-1.52) *Npy1r* # (-1.56, -1.36) *Stat1* * (-1.32) *Plat* # (-1.36, -1.23) *Stat6* * (-1.32) *Ppih* * (-1.35) *Actb* * (-1.24) *Nono* # (-1.50, -1.97)

Table 12 Gene markers that are up-regulated and down-regulated in the male S-fluoxetine group versus male R-fluoxetine group. At the top of the table, genes with *P*-values less than 0.05 are shown. At the bottom of the table, any gene which changes more than 2 fold is also considered a significant change (highlighted in yellow). Rest of the gene markers are not statistically significant. # denotes both replicates of the gene, and * denotes one of the two replicates of the gene. The blue line demarcates statistical significance: gene markers listed above are statistically significant and those listed below are statistically insignificant as far as the *P*-value goes only. Fold-regulation for each gene marker is indicated in brackets.

As seen in figure 25, the male group treated with S-fluoxetine is compared against the male R-fluoxetine group. Both groups comprise of five rats. The graph indicates *Sox2*, *Nono*, and *Grip1* as statistically significant and are down-regulated (green), while *Nos2* is also statistically significant and is up-regulated (red). Decreased *Sox2* indicates lowered stem cell maintenance, while *Grip1* affecting cellular signaling and *Nono* affecting the gene transcription. Increased levels of *Nos2* indicates more of the M1 pro-inflammatory microglia present in the male R-fluoxetine group compared to their S-

fluoxetine counterpart. Horizontal blue line on the graph divides the above gene markers as statistically significant with *P*-value less than 0.05, and those below are statistically insignificant with *P*-value greater than 0.05. Gene markers plotted on both sides of the pink vertical lines are significant with changes more than 2-fold.

Table 12 lists several gene markers that are up-regulated and down-regulated in the comparison of male S-fluoxetine versus male R-fluoxetine groups. *Il6* is significantly up-regulated indicating either M1 pro-inflammatory or M2b anti-inflammatory microglial activation. Other markers were non-significant and up-regulated including *Crh*, *Crhr2*, *Stat4*, *Cd40*, and *Fos*.

Cbln1 is significant and down-regulated with change of more than 2-fold. Others are non-significant and down-regulated which include growth factors such as *Bdnf*, *Cntf*, *Cntfr*, and *Npy1r*; cam-kinases such as *Camk2a* and *Camk2g*; others such as *Galr1*, *Gfra3*, *Actb*, and *Il-10ra*; and additionally microglial markers such as *Stat11*, *Ccl11*, *Cd163*, and *Stat6*. Also down-regulated were markers such as *Crhbp*, *Plat*, *Nono*, *Ppih*.

Gene Markers of Microglial Subtypes

Microglia are brain resident macrophages which are activated upon stroke to prevent further neurological damage. In that process, four subtypes of microglia are studied in this project from the peri-infarct region to understand their role in inflammation. The M1 subtype is pro-inflammatory microglia, while the M2 subtype is an anti-inflammatory microglia. M2 subtype comprises of three categories: M2a, M2b, and M2c, where M2a and M2c are strictly non-inflammatory, while M2b qualifies as a pro-inflammatory with majority of its gene markers except for one gene marker of Interleukin-10 (*Il-10*) that puts it into the M2 anti-inflammatory microglial subtype. In

this part of study, Ct-values obtained from real-time polymerase chain reaction are plotted to simply compare and contrast the gene markers of certain subtype of microglia at a given time in the cycle. Threshold was manually set the same across all groups in all RT-PCR plates that were tested.

For the purpose to purely identify which microglia is or are activated after stroke, they are plotted in graphs in figure 26. Visible in all four graphs, all four microglial subtypes were present after stroke induction, and they are all expressed in the same linear proportion range of Ct. This part of project is simply carried out to assess which proposed microglial subtypes participate in the brain peri-infarct region to induce pro-inflammation and/or anti-inflammation. Refer to the volcano plots in the Gene Expression Analysis section to discover whether or not the treatment of FDA approved drugs activate or inhibit the response of any of the four microglial subtypes demonstrated in the following graph, with any remarkable change in Ct-values.

Control Group

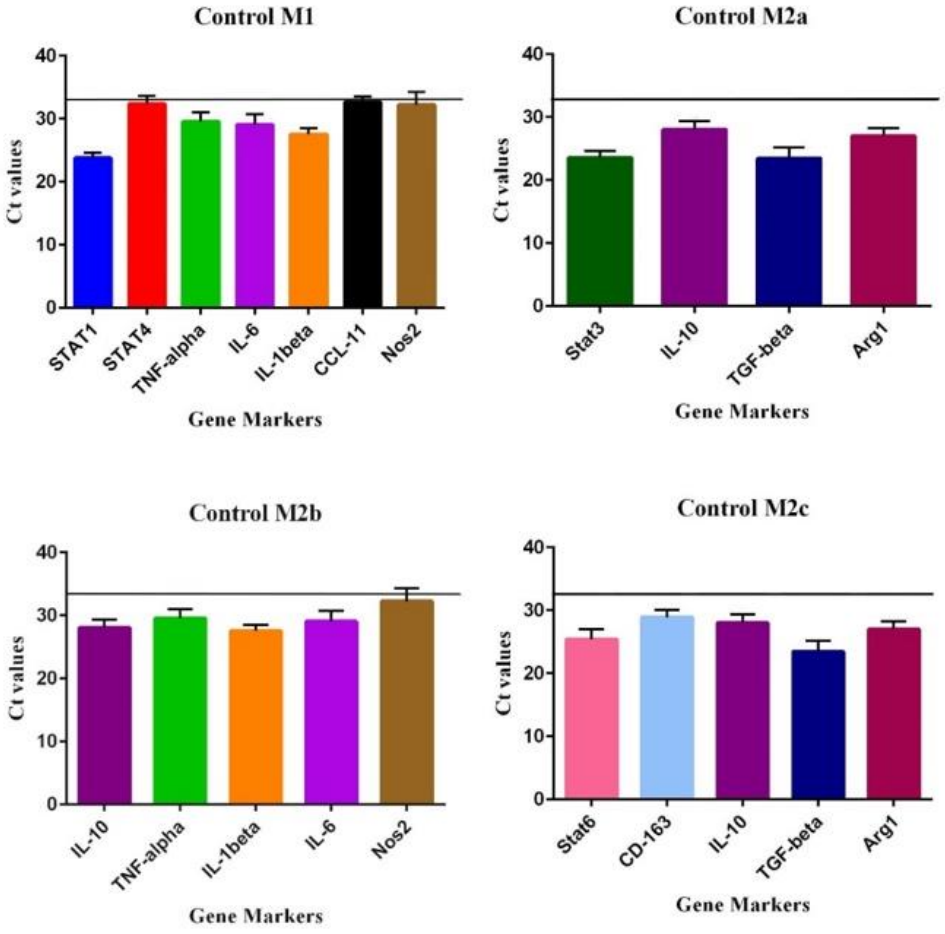

Figure 26 Microglial gene markers (M1, M2a, M2b, M2c) distinguished in the Control group

IV. DISCUSSION

Motor Functional Analysis

Contralateral functional deficit of greater than or equal to 20% was required criteria to include animals in the analysis of motor function. Endothelin-1, a potent vasoconstrictor was introduced into the right hemisphere of brain to induce stroke in aged, 10-12 months old Sprague Dawley rats. The resulting stroke in the forelimb motor cortex of the right hemisphere in Sprague Dawley rats made their left (contralateral) side deficient compared to their pre-stroke function. Six different groups were treated with FDA approved drugs: female FSA (fluoxetine, simvastatin, ascorbic acid) group (abbreviated FFSA), male (MS-fluox) and female (FS-fluox) groups with S-fluoxetine (and simvastatin plus ascorbic acid), male (MR-fluox) and female (FR-fluox) groups with R-fluoxetine (and simvastatin plus ascorbic acid), and female control (FC) group (placebo, no drugs). Average contralateral baseline function deficit in each group resulted as follows: FC – 72%, FFSA – 84%, FS-fluoxetine – 80%, FR-fluoxetine – 77%, MS-fluoxetine – 54%, MR-fluoxetine – 57%. No statistically significant difference was noted between the female Montoya groups (FC, FFSA, FS-fluoxetine, and FR-fluoxetine) or between the male Montoya groups (MS-fluoxetine and MR-fluoxetine). There does appear to be a difference between males and the females, but that was probably because the males had a larger infarct volume. In this project, we were only interested in baseline contralateral function to indicate that stroke did occur by ensuring their motor function

was reduced; we were not interested in their motor functional recovery however because that would require prolonged treatment with drugs, whereas, we had to sacrifice the rats on 7th day in order to study gene expression of microglial subtypes and growth factors involved early in the disease stages. We did not examine the infarct volume in these animals, as we excised the peri-infarct region for our gene expression studies. Although some rats in certain groups were excluded due to failure to pass the criteria for the motor functional study, they are all included in the Evans Blue analysis and gene expression studies to follow because of the confirmed presence of an infarct in the right hemisphere.

Evans Blue BBB Permeability

Evans Blue dye permeability in the cerebral cortex (P=0.0041) as well as in the cerebellum (P=0.0423) of female group treated with S-fluoxetine was significantly less compared to male group treated with R-fluoxetine. Within the male rats, Evans Blue permeability in the cerebral cortex (P=0.0045) was significantly reduced in the presence of the S-fluoxetine compared to the R-fluoxetine. Therefore, the S-fluoxetine appears to tighten the blood brain barrier in both males and females, while the R-fluoxetine data in males show an enhanced permeability. There is also a statistical difference present in the cerebellum of female R-fluoxetine compared to male R-fluoxetine, as confirmed by an unpaired t-test with Welch's correction (P=0.0407). This allows us to deduce that S-fluoxetine tightens the blood brain barrier (BBB), preventing its disruption in the male and female group while R-fluoxetine allows the dye to cross the BBB. Since the R-fluoxetine shows a significant increase in the BBB permeability in female versus male group, our data suggests that the R- fluoxetine is less effective to guard the BBB against damage following stroke compared to S-fluoxetine in both sexes. However, we did not

see a statistical difference in Evans Blue permeation when S-fluoxetine was compared to R-fluoxetine in females, but that may have been due to limited perfusion time for the Evans Blue (see below).

In this experiment we had very limited exposure to Evans Blue in the circulation before it was washed out, which has complicated interpretation of the results. The trichloroacetic method of Evans Blue assay applied in this project to study its permeability has been previously confirmed to be working in limited rat tissue samples *in vivo* and *in vitro* in small rodent models [56].

So, why is there a difference between the R and S enantiomers of fluoxetine in only some but not all of the male and female groups. As mentioned above, we saw a permeability difference between male groups but not between female groups. One explanation could be due to the fact that animals were perfused with Evans Blue dye for less than 10 minutes, which is considerably a short period of time. Instead, longer perfusion for approximately 10 to 30 minutes would probably make a difference in allowing permeation at the BBB in all groups of rats tested. In other literature in the field, a two hour Evans Blue perfusion was used when evaluating if the drug etoposide can prevent blood brain barrier disruption in Sprague Dawley rats [81]. An Evans blue study in 8 months old CD1 mice perfused for 3 hours shows 10mg/kg fluoxetine treatment blocked BBB disruption in the Hippocampus after ischemia and also prevented infiltration of macrophages to inhibit inflammatory mediators after injury [82].

Another explanation could be due to the drugs working along different pathways in male and female Sprague Dawley rats, showing a gender difference response. Fluoxetine has been shown in adult mice to have some gender differences in alterations

of neuronal cell proliferation and survival in multiple regions of the brain [83]. We also see some statistical differences between female and male rats exposed to the same drugs post-stroke in our analysis of gene expression differences.

Gene Markers of the Microglial Subtypes

Our results show there is a notable difference between the effects of administration of R- and S-enantiomers of fluoxetine on microglial subtypes genes expressed in male and female Sprague Dawley rats. Our results indicate that the R-fluoxetine treatment in female group increased anti-inflammation by up-regulating M2 gene expression (both replicates of *Arg1* suggesting M2a or M2c subtype), while that in male group increased pro-inflammation by up-regulating M1 microglial gene expression, as when both are compared within their own gender with S-fluoxetine. The treatment of R-fluoxetine in male compared against female showed a strong decrease in anti-inflammation by down-regulating M2 microglial gene markers (both replicates of *Arg1* and *Cd163* suggesting M2c subtype). Our results also indicate that the FSA and S-fluoxetine treatment in female groups up-regulated several growth factors contributing to neurogenesis after stroke, however, the results were statistically insignificant in the S-fluoxetine treatment group; we might try increasing our animal numbers in the next tests to see if we can gain significance. R-fluoxetine treatment in female compared against female S-fluoxetine, showed down-regulation of growth factors, which again was not statistically significant in these preliminary studies.

Several growth factors are significantly up-regulated, but we also see a down-regulation of *Arg1*; this suggests that either the microglial markers chosen in this project do not correspond to the subtypes of macrophages in the periphery, or the increase in

Bdnf is not due to microglial polarization. Some of the genes are linked such as *Npy1r*, *Bdnf*, and stress markers, which suggests a possibility that *Bdnf* may be up-regulated through Orexin pathways distributed in a rat brain [84]. Or it may be because microglial markers are possibly be showing sex and age dependent changes.

Most studies in the field have not looked at differences in the microglial response to stroke for both male and female rats. For example, a study that first identified that M1 and M2 subtypes have different functions in neurodegenerative disease, was only performed in males [85]. In this study, the M1 subtype is triggered at the end stage of the disease when the M2 therapeutic subtype is suppressed. The M1 subtype therefore is widely known as the terminal inflammatory microglia that destroys the tissue, while the M2 subtype provides healing immune markers at the site of injury to salvage and recover from persisting neurological damage. In a stroke, however, we expect to see most of the damage and inflammatory microglia infiltration beginning 24 hours after stroke induction. So, in this study, by waiting for 7 days after stroke, any M1 microglia in our control and treated animals may have cycled into M2 types, so that we don't see distinct drug effects on control versus fluoxetine treatments.

Other work in the field has also found that M2 subtype microglia can be pro-tumorigenic in neurofibromatosis and that macrophages had a direct effect on neurofibroma tumor formation and growth [86]. Therefore, it might not be beneficial to keep patients on a drug that promotes M2 microglia for a long period of time, but this would have to be investigated with longer periods of recovery.

It is also possible that the inflammatory related responses occurring at early stages in an animal model dramatically progressed and modulated (activated or inhibited) at

advanced stages in the disease. It has been shown in 10 week old C57BI/6 male mice that a specific phenotype of microglia activation presented distinct spatial and temporal features meaning it depends on surrounding micro-environmental signals that can change over time. This study thereby showed that microglial subtypes are cycle dependent and their response may evolve with time and location [87]. Another study reveals polarization of M2a microglia phenotype by *Il-4* depends on specific area of the brain, showing reduced M2a response in striatum compared to frontal cortex [74]. In this study, *Il-4* was injected centrally in the third cerebral ventricle of mice brain to induce polarization. Note that all of the ventricles are connected in the brain, and the general flow is toward the anterior cortex, so any drug injected into the ventricle would be expected to have its strongest effect in the anterior cortex.

It has been recently discovered that differences in microglia and cytokines produced are crucial for sexual differentiation of brain and behavior in early development in Sprague Dawley rats. This study proves a sex-specific brain development due to testosterone up-regulating the pro-inflammatory molecule called prostaglandin-E2, which is released from microglia [88]. We also see some sex differences in the brain's response to certain drugs, (see volcano plots), where a particular type of microglia is either up or down-regulated. These differences may be due to the "masculinization of the brain" seen in Dr. McCarthy's lab, which appears to be based on microglial differences rather than direct hormone differences [88].

There is an indication in our results of down-regulated M1 microglial gene markers including *Tnf-alpha*, *Il-6*, *Il1-beta*, *Ccl11*, *Stat1*, *Stat4*, and *Nos2* showing decreased pro-inflammation due to R-fluoxetine; however, these results were statistically

insignificant in this preliminary data. A number of other studies in the field do affirm down-regulated pro-inflammation genes. A 2015 study indicates fluoxetine and S-citalopram caused down-regulation of M1 and up-regulation of M2 microglial activation to modulate anti-depressant effects. This was measured using real-time PCR, as was our study, but performed *in vitro* microglial cultures [64].

Another *in-vitro* study showed that fluoxetine significantly inhibited TNF-alpha, nitric oxide (NO), and *Il-6* thereby producing anti-inflammatory effects, which again is similar to our finding [89]. However, an *in-vitro* study is not strictly comparable to an *in-vivo* study due to the fact that fluoxetine gets metabolized *in vivo* to a nor-fluoxetine form. The S-norfluoxetine form is active, while the R-norfluoxetine form is not, and our previous work shows that norfluoxetine can stay elevated in the brain over a week after delivery [15].

Another microglial cell culture study indicates fluoxetine is able to inhibit microglial *Tnf-alpha* and NO production, mediating anti-inflammatory effects through cAMP signaling pathway [71]. Certainly, this was not the case discovered in our results performed *in vivo*. Our results have shown that *Creb1*, which is activated by the cAMP pathways was up- or down-regulated similar to the pro-inflammatory markers results in the groups tested. It was discovered on the same side of up- or down-regulation as for the pro-inflammatory M1 markers. This contradiction is probably due to the fluoxetine metabolism *in vivo*.

A BV2 microglial cell culture demonstrates fluoxetine significantly inhibited *Tnf-alpha*, *Il-6*, and NO from LPS-activated microglia [90]. Another *in vitro* study confirms fluoxetine significantly inhibited *Tnf-alpha*, *Il-1beta*, and NO which are pro-

inflammatory cytokines, thereby mediating neuro-protection. Both R- and S- enantiomers of fluoxetine were tested and showed microglia-dependent neuroprotection [66]. Both enantiomers of fluoxetine are active, so no real differences would be expected *in vitro*.

A study in male Wistar rats indicates pro-inflammatory *Il1-beta* reduction in the pre-frontal cortex by fluoxetine is how it exerts its anti-inflammatory properties [91]. This is also identified in our results that the R-fluoxetine in male group compared to female control group, and both R- and S-fluoxetine in female group compared to male and female control groups, showed down-regulation of *Il1-beta*. This particular cytokine is a primary key factor which recruits other M1 microglial gene markers to induce pro-inflammation, therefore, if *Il1-beta* is decreased, then certainly pro-inflammation is decreased all together, particularly due to R-fluoxetine as discovered in our present study.

We also see a significant up-regulation of Cerebellin-1 (*Cbln1*) in female groups treated with both fluoxetine enantiomers. This particular cerebellum-specific protein is involved in controlling neuroplasticity and synaptic structure by playing a role in neuronal signaling pathway [92]. It is implicated in pre-synapse formation at the axon terminals which form axodendritic synapses in striatal medium spiny neurons [93]. This may also aide in stabilizing the active zone in sub-ventricular region focused in our study where neuronal signaling can be passed from dendrites to axon.

V. CONCLUSION AND FUTURE STUDIES

While the fluoxetine (Prozac) in our drug combination has been beneficial to improve neurogenesis in our stroke studies, our results suggest that the S-enantiomer of fluoxetine may be more beneficial therapeutically. The blood brain barrier showed less permeability to Evans Blue dye due to S-fluoxetine, which may possibly have been implicated in tightening the BBB compared to the R-enantiomer. In future studies on the Evans Blue permeability across the BBB, we shall consider increasing the time allowed for perfusion (longer than 10 minutes allowed in this preliminary study); this may possibly enable us to see perfusion across all animal groups we had chosen for the analysis.

In the gene expression studies, our results indicated that the S-enantiomer of fluoxetine up-regulated neurogenesis growth factors and neuroplasticity factors compared to R-fluoxetine. Also, our chosen neuro-inflammatory cytokine markers were also notably present in this part of the project, which indicates a possible role of fluoxetine enantiomers in neuro-inflammation after stroke. In future studies on the gene expression, we might gain more significance across the groups studied by increasing the number of male and female animals; this would enable us to identify significant gene markers that could be targeted for therapeutic treatment after stroke.

VI. REFERENCES

1. Mozaffarian, D., et al., *Heart disease and stroke statistics--2015 update: a report from the American Heart Association.* Circulation, 2015. **131**(4): p. e29-322.
2. Meschia, J.F., et al., *Guidelines for the primary prevention of stroke: a statement for healthcare professionals from the American Heart Association/American Stroke Association.* Stroke, 2014. **45**(12): p. 3754-832.
3. Hall, M.J., S. Levant, and C.J. DeFrances, *Hospitalization for stroke in U.S. hospitals, 1989-2009.* NCHS Data Brief, 2012(95): p. 1-8.
4. Del Zoppo, G.J., et al., *Expansion of the time window for treatment of acute ischemic stroke with intravenous tissue plasminogen activator: a science advisory from the American Heart Association/American Stroke Association.* Stroke, 2009. **40**(8): p. 2945-8.
5. Barber, P.A., et al., *Why are stroke patients excluded from TPA therapy? An analysis of patient eligibility.* Neurology, 2001. **56**(8): p. 1015-1020.
6. Ribo, M., et al., *Maximal Admission Core Lesion Compatible With Favorable Outcome in Acute Stroke Patients Undergoing Endovascular Procedures.* Stroke, 2015. **46**(10): p. 2849-2852.
7. Hankey, G.J. and J.W. Eikelboom, *Antithrombotic drugs for patients with ischaemic stroke and transient ischaemic attack to prevent recurrent major vascular events.* Lancet Neurol, 2010. **9**(3): p. 273-84.
8. Brekenfeld, C., et al., *Mechanical Thrombectomy for Acute Ischemic Stroke.* Rofo-Fortschritte Auf Dem Gebiet Der Rontgenstrahlen Und Der Bildgebenden Verfahren, 2012. **184**(6): p. 503-512.
9. Corbett, A.M., et al., *Increasing neurogenesis with fluoxetine, simvastatin and ascorbic Acid leads to functional recovery in ischemic stroke.* Recent Pat Drug Deliv Formul, 2015. **9**(2): p. 158-66.
10. Malberg, J.E., et al., *Chronic antidepressant treatment increases neurogenesis in adult rat hippocampus.* J Neurosci, 2000. **20**(24): p. 9104-10.
11. Lu, D., et al., *Statins increase neurogenesis in the dentate gyrus, reduce delayed neuronal death in the hippocampal CA3 region, and improve spatial learning in rat after traumatic brain injury.* J Neurotrauma, 2007. **24**(7): p. 1132-46.
12. Sett, A.K., T.G. Robinson, and A.K. Mistri, *Current status of statin therapy for stroke prevention.* Expert Rev Cardiovasc Ther, 2011. **9**(10): p. 1305-14.
13. Garcia-Bonilla, L., et al., *Evidence for the efficacy of statins in animal stroke models: a meta-analysis.* J Neurochem, 2012. **122**(2): p. 233-43.
14. Cui, X., et al., *Therapeutic benefit of treatment of stroke with simvastatin and human umbilical cord blood cells: neurogenesis, synaptic plasticity, and axon growth.* Cell Transplant, 2012. **21**(5): p. 845-56.
15. Corbett, A., et al., *A method for reliable voluntary oral administration of a fixed dosage (mg/kg) of chronic daily medication to rats.* Lab Anim, 2012. **46**(4): p. 318-24.

16. Chen, J., et al., *Endothelial nitric oxide synthase regulates brain-derived neurotrophic factor expression and neurogenesis after stroke in mice.* J Neurosci, 2005. **25**(9): p. 2366-75.
17. Szczepanska-Szerej, A., et al., *Simvastatin displays an antioxidative effect by inhibiting an increase in the serum 8-isoprostane level in patients with acute ischemic stroke: brief report.* Clin Neuropharmacol, 2011. **34**(5): p. 191-4.
18. Mostert, J.P., et al., *Therapeutic potential of fluoxetine in neurological disorders.* CNS Neurosci Ther, 2008. **14**(2): p. 153-64.
19. Mikami, K., et al., *Effect of antidepressants on the course of disability following stroke.* Am J Geriatr Psychiatry, 2011. **19**(12): p. 1007-15.
20. Chollet, F., et al., *Fluoxetine for motor recovery after acute ischaemic stroke (FLAME): a randomised placebo-controlled trial.* Lancet Neurol, 2011. **10**(2): p. 123-30.
21. Cramer, S.C., *Listening to fluoxetine: a hot message from the FLAME trial of poststroke motor recovery.* Int J Stroke, 2011. **6**(4): p. 315-6.
22. Narushima, K., et al., *Effect of antidepressant therapy on executive function after stroke.* Br J Psychiatry, 2007. **190**: p. 260-5.
23. Ng, K.L., et al., *Fluoxetine Maintains a State of Heightened Responsiveness to Motor Training Early After Stroke in a Mouse Model.* Stroke, 2015. **46**(10): p. 2951-60.
24. Sun, X., et al., *Fluoxetine enhanced neurogenesis is not translated to functional outcome in stroke rats.* Neurosci Lett, 2015. **603**: p. 31-6.
25. Berends, H.I., et al., *Single dose of fluoxetine increases muscle activation in chronic stroke patients.* Clin Neuropharmacol, 2009. **32**(1): p. 1-5.
26. Li, W.L., et al., *Chronic fluoxetine treatment improves ischemia-induced spatial cognitive deficits through increasing hippocampal neurogenesis after stroke.* J Neurosci Res, 2009. **87**(1): p. 112-22.
27. Sas, K., et al., *Effects of citalopram and fluoxetine on the corticocerebral blood flow in conscious rabbits.* Acta Physiol Hung, 2007. **94**(3): p. 167-77.
28. Sit, D., et al., *Disposition of chiral and racemic fluoxetine and norfluoxetine across childbearing.* J Clin Psychopharmacol, 2010. **30**(4): p. 381-6.
29. Wong, D.T., L.R. Reid, and P.G. Threlkeld, *Suppression of food intake in rats by fluoxetine: comparison of enantiomers and effects of serotonin antagonists.* Pharmacol Biochem Behav, 1988. **31**(2): p. 475-9.
30. Whirl-Carrillo, M., et al., *Pharmacogenomics knowledge for personalized medicine.* Clin Pharmacol Ther, 2012. **92**(4): p. 414-7.
31. Jannuzzi, G., et al., *Plasma concentrations of the enantiomers of fluoxetine and norfluoxetine: sources of variability and preliminary observations on relations with clinical response.* Ther Drug Monit, 2002. **24**(5): p. 616-27.
32. Magyar, J., et al., *Differential effects of fluoxetine enantiomers in mammalian neural and cardiac tissues.* Int J Mol Med, 2003. **11**(4): p. 535-42.
33. Altamura, A.C., A.R. Moro, and M. Percudani, *Clinical pharmacokinetics of fluoxetine.* Clin Pharmacokinet, 1994. **26**(3): p. 201-14.

34. Spratt, N.J., et al., *Modification of the method of thread manufacture improves stroke induction rate and reduces mortality after thread-occlusion of the middle cerebral artery in young or aged rats.* J Neurosci Methods, 2006. **155**(2): p. 285-90.
35. Park, S.Y., et al., *A method for generating a mouse model of stroke: evaluation of parameters for blood flow, behavior, and survival [corrected].* Exp Neurobiol, 2014. **23**(1): p. 104-14.
36. Fluri, F., M.K. Schuhmann, and C. Kleinschnitz, *Animal models of ischemic stroke and their application in clinical research.* Drug Des Devel Ther, 2015. **9**: p. 3445-54.
37. Maynard, K.I., et al., *The acoustic startle reflex in Sprague-Dawley rats is altered by permanent middle cerebral artery occlusion.* Brain Res, 2005. **1032**(1-2): p. 44-9.
38. Belayev, L., et al., *Middle cerebral artery occlusion in the rat by intraluminal suture. Neurological and pathological evaluation of an improved model.* Stroke, 1996. **27**(9): p. 1616-22; discussion 1623.
39. Carmichael, S.T., *Rodent models of focal stroke: size, mechanism, and purpose.* NeuroRx, 2005. **2**(3): p. 396-409.
40. Jin, K., et al., *Delayed transplantation of human neural precursor cells improves outcome from focal cerebral ischemia in aged rats.* Aging Cell, 2010. **9**(6): p. 1076-83.
41. Labat-gest, V. and S. Tomasi, *Photothrombotic ischemia: a minimally invasive and reproducible photochemical cortical lesion model for mouse stroke studies.* J Vis Exp, 2013(76).
42. Warner-Schmidt, J.L. and R.S. Duman, *Hippocampal neurogenesis: opposing effects of stress and antidepressant treatment.* Hippocampus, 2006. **16**(3): p. 239-49.
43. Lee, J.C., et al., *Voluntary wheel running reverses the decrease in subventricular zone neurogenesis caused by corticosterone.* Cell Transplant, 2016.
44. Abdanipour, A., et al., *In vitro study of the long-term cortisol treatment effects on the growth rate and proliferation of the neural stem/precursor cells.* Neurol Res, 2015. **37**(2): p. 117-24.
45. Acosta, S.A., et al., *Influence of post-traumatic stress disorder on neuroinflammation and cell proliferation in a rat model of traumatic brain injury.* PLoS One, 2013. **8**(12): p. e81585.
46. Cavaliere, F., M. Benito-Munoz, and C. Matute, *Organotypic Cultures as a Model to Study Adult Neurogenesis in CNS Disorders.* Stem Cells Int, 2016. **2016**: p. 3540568.
47. Aguilera, G., A. Kiss, and B. Sunar-Akbasak, *Hyperreninemic hypoaldosteronism after chronic stress in the rat.* J Clin Invest, 1995. **96**(3): p. 1512-9.
48. Alme, M.N., et al., *Chronic fluoxetine treatment induces brain region-specific upregulation of genes associated with BDNF-induced long-term potentiation.* Neural Plast, 2007. **2007**: p. 26496.
49. Nagai, K., T. Inoue, and H. Konishi, *Increased gene expression of glucose transporters in the mouse brain after treatment with fluoxetine and pergolide.* Drug Res (Stuttg), 2014. **64**(7): p. 389-91.

50. Johnson-Anuna, L.N., et al., *Chronic administration of statins alters multiple gene expression patterns in mouse cerebral cortex.* J Pharmacol Exp Ther, 2005. **312**(2): p. 786-93.
51. Chen, J., et al., *Statins induce angiogenesis, neurogenesis, and synaptogenesis after stroke.* Ann Neurol, 2003. **53**(6): p. 743-51.
52. Bracko, O., et al., *Gene expression profiling of neural stem cells and their neuronal progeny reveals IGF2 as a regulator of adult hippocampal neurogenesis.* J Neurosci, 2012. **32**(10): p. 3376-87.
53. Ferron, S.R., et al., *Differential genomic imprinting regulates paracrine and autocrine roles of IGF2 in mouse adult neurogenesis.* Nat Commun, 2015. **6**: p. 8265.
54. Shigemoto-Mogami, Y., et al., *Microglia enhance neurogenesis and oligodendrogenesis in the early postnatal subventricular zone.* J Neurosci, 2014. **34**(6): p. 2231-43.
55. da Fonseca, A.C., et al., *The impact of microglial activation on blood-brain barrier in brain diseases.* Front Cell Neurosci, 2014. **8**: p. 362.
56. Wang, H.L. and T.W. Lai, *Optimization of Evans blue quantitation in limited rat tissue samples.* Sci Rep, 2014. **4**: p. 6588.
57. Kitamura, Y., et al., *Recovery of focal brain ischemia-induced behavioral dysfunction by intracerebroventricular injection of microglia.* J Pharmacol Sci, 2005. **97**(2): p. 289-93.
58. Foey, A.D. and S. Crean, *Macrophage subset sensitivity to endotoxin tolerisation by Porphyromonas gingivalis.* PLoS One, 2013. **8**(7): p. e67955.
59. Foey, A.D., *Macrophages — Masters of Immune Activation, Suppression and Deviation.* InTech, 2014. **Immunology and Microbiology**("Immune Response Activation").
60. Varnum, M.M. and T. Ikezu, *The classification of microglial activation phenotypes on neurodegeneration and regeneration in Alzheimer's disease brain.* Arch Immunol Ther Exp (Warsz), 2012. **60**(4): p. 251-66.
61. Morganti, J.M., L.K. Riparip, and S. Rosi, *Call Off the Dog(ma): M1/M2 Polarization Is Concurrent following Traumatic Brain Injury.* PLoS One, 2016. **11**(1): p. e0148001.
62. Tang, Y. and W. Le, *Differential Roles of M1 and M2 Microglia in Neurodegenerative Diseases.* Mol Neurobiol, 2015.
63. Xia, C.Y., et al., *Selective modulation of microglia polarization to M2 phenotype for stroke treatment.* Int Immunopharmacol, 2015. **25**(2): p. 377-82.
64. Su, F., et al., *Fluoxetine and S-citalopram inhibit M1 activation and promote M2 activation of microglia in vitro.* Neuroscience, 2015. **294**: p. 60-8.
65. Lim, C.M., et al., *Fluoxetine affords robust neuroprotection in the postischemic brain via its anti-inflammatory effect.* J Neurosci Res, 2009. **87**(4): p. 1037-45.
66. Zhang, F., et al., *Fluoxetine protects neurons against microglial activation-mediated neurotoxicity.* Parkinsonism Relat Disord, 2012. **18 Suppl 1**: p. S213-7.
67. Dhami, K.S., et al., *Fluoxetine and citalopram decrease microglial release of glutamate and D-serine to promote cortical neuronal viability following ischemic insult.* Mol Cell Neurosci, 2013. **56**: p. 365-74.

68. Lee, J.Y., S.R. Kang, and T.Y. Yune, *Fluoxetine prevents oligodendrocyte cell death by inhibiting microglia activation after spinal cord injury.* J Neurotrauma, 2015. **32**(9): p. 633-44.
69. Zychowska, M., et al., *The influence of microglia activation on the efficacy of amitriptyline, doxepin, milnacipran, venlafaxine and fluoxetine in a rat model of neuropathic pain.* Eur J Pharmacol, 2015. **749**: p. 115-23.
70. Yang, J.M., et al., *Acetylsalicylic acid enhances the anti-inflammatory effect of fluoxetine through inhibition of NF-kappaB, p38-MAPK and ERK1/2 activation in lipopolysaccharide-induced BV-2 microglia cells.* Neuroscience, 2014. **275**: p. 296-304.
71. Tynan, R.J., et al., *A comparative examination of the anti-inflammatory effects of SSRI and SNRI antidepressants on LPS stimulated microglia.* Brain Behav Immun, 2012. **26**(3): p. 469-79.
72. Orio, L., et al., *3,4-Methylenedioxymethamphetamine increases interleukin-1beta levels and activates microglia in rat brain: studies on the relationship with acute hyperthermia and 5-HT depletion.* J Neurochem, 2004. **89**(6): p. 1445-53.
73. Churchward, M.A. and K.G. Todd, *Statin treatment affects cytokine release and phagocytic activity in primary cultured microglia through two separable mechanisms.* Mol Brain, 2014. **7**: p. 85.
74. Pepe, G., et al., *Heterogeneous induction of microglia M2a phenotype by central administration of interleukin-4.* J Neuroinflammation, 2014. **11**: p. 211.
75. Hou, Y.C., et al., *Preventive effect of silymarin in cerebral ischemia-reperfusion-induced brain injury in rats possibly through impairing NF-kappaB and STAT-1 activation.* Phytomedicine, 2010. **17**(12): p. 963-73.
76. Wen, T.C., et al., *Induction of phosphorylated-Stat3 following focal cerebral ischemia in mice.* Neurosci Lett, 2001. **303**(3): p. 153-6.
77. Lin, H.W. and S.W. Levison, *Context-dependent IL-6 potentiation of interferon- gamma-induced IL-12 secretion and CD40 expression in murine microglia.* J Neurochem, 2009. **111**(3): p. 808-18.
78. Hoffmann, C.J., et al., *Vascular signal transducer and activator of transcription-3 promotes angiogenesis and neuroplasticity long-term after stroke.* Circulation, 2015. **131**(20): p. 1772-82.
79. Manwani, B., et al., *Differential effects of aging and sex on stroke induced inflammation across the lifespan.* Exp Neurol, 2013. **249**: p. 120-31.
80. Dinapoli, V.A., et al., *Age exaggerates proinflammatory cytokine signaling and truncates signal transducers and activators of transcription 3 signaling following ischemic stroke in the rat.* Neuroscience, 2010. **170**(2): p. 633-44.
81. Spigelman, M.K., et al., *Etoposide induced blood-brain barrier disruption in rats: duration of opening and histological sequelae.* Cancer Res, 1986. **46**(3): p. 1453-7.
82. Lee, J.Y., et al., *Fluoxetine inhibits transient global ischemia-induced hippocampal neuronal death and memory impairment by preventing blood-brain barrier disruption.* Neuropharmacology, 2014. **79**: p. 161-71.

83. Hodes, G.E., et al., *Sex-specific effects of chronic fluoxetine treatment on neuroplasticity and pharmacokinetics in mice.* J Pharmacol Exp Ther, 2010. **332**(1): p. 266-73.
84. Holland, P. and P.J. Goadsby, *The hypothalamic orexinergic system: pain and primary headaches.* Headache, 2007. **47**(6): p. 951-62.
85. Tang, Y. and W. Le, *Differential Roles of M1 and M2 Microglia in Neurodegenerative Diseases.* Mol Neurobiol, 2016. **53**(2): p. 1181-94.
86. Prada, C.E., et al., *Neurofibroma-associated macrophages play roles in tumor growth and response to pharmacological inhibition.* Acta Neuropathol, 2013. **125**(1): p. 159-68.
87. Perego, C., S. Fumagalli, and M.G. De Simoni, *Temporal pattern of expression and colocalization of microglia/macrophage phenotype markers following brain ischemic injury in mice.* J Neuroinflammation, 2011. **8**: p. 174.
88. Lenz, K.M., et al., *Microglia are essential to masculinization of brain and behavior.* J Neurosci, 2013. **33**(7): p. 2761-72.
89. Du, R.W., R.H. Du, and W.G. Bu, *beta-Arrestin 2 mediates the anti-inflammatory effects of fluoxetine in lipopolysaccharide-stimulated microglial cells.* J Neuroimmune Pharmacol, 2014. **9**(4): p. 582-90.
90. Liu, D., et al., *Anti-inflammatory effects of fluoxetine in lipopolysaccharide(LPS)-stimulated microglial cells.* Neuropharmacology, 2011. **61**(4): p. 592-9.
91. Pan, Y., et al., *Microglial NLRP3 inflammasome activation mediates IL-1beta-related inflammation in prefrontal cortex of depressive rats.* Brain Behav Immun, 2014. **41**: p. 90-100.
92. Hirai, H., et al., *Cbln1 is essential for synaptic integrity and plasticity in the cerebellum.* Nat Neurosci, 2005. **8**(11): p. 1534-41.
93. Kusnoor, S.V., et al., *Extracerebellar role for Cerebellin1: modulation of dendritic spine density and synapses in striatal medium spiny neurons.* J Comp Neurol, 2010. **518**(13): p. 2525-37.